Copyright Warning & Restrictions

The copyright law of the United States (Title 17, United States Code) governs the making of photocopies or other reproductions of copyrighted material.

Under certain conditions specified in the law, libraries and archives are authorized to furnish a photocopy or other reproduction. One of these specified conditions is that the photocopy or reproduction is not to be "used for any purpose other than private study, scholarship, or research." If a, user makes a request for, or later uses, a photocopy or reproduction for purposes in excess of "fair use" that user may be liable for copyright infringement,

This institution reserves the right to refuse to accept a copying order if, in its judgment, fulfillment of the order would involve violation of copyright law.

Please Note: The author retains the copyright while the New Jersey Institute of Technology reserves the right to distribute this thesis or dissertation

Printing note: If you do not wish to print this page, then select "Pages from: first page # to: last page #" on the print dialog screen

NJIT New Jersey's Science & Technology University

The Van Houten library has removed some of the personal information and all signatures from the approval page and biographical sketches of theses and dissertations in order to protect the identity of NJIT graduates and faculty.

ABSTRACT

Modification of Wear Testing Machine and Study of Wear Resistance

Ning Li

In this work a modification of a wear testing machine has been done by designing a new loading mechanism and redesigning different components for a new roller-on-roller wear testing machine. A new loading mechanism containing gearbox frame and load cell assembly have been designed, manufactured and assembled. A pusher of the pushing mechanism is redesigned for better durability. Existing bearing support was redesigned and replaced. All new units of the wear testing machine were lined up and assembled with the machine. Finite element stress analysis for designed frame in the load mechanism was performed by using the Integrate Design Engineering Assistant System, known as I-Deas, and ANSYS.

More than 30 AISI D2 and H13 tool steel specimens treated by plasma ion nitriding and/or magnetic treatment were tested on a computer controlled wear testing machine. The operational surface roughness has been investigated during all stages of wear. It was found that plasma ion nitriding surface treatment improves the wear resistance of the tool steel dramatically. The higher the nitrogen concentration is used the better the improvement is. Specimens treated with higher nitrogen concentration provide better wear resistance. Surface treated by a combination of processes: ion nitriding and magnetization improve wear resistance. Magnetic treatment applied before ion nitriding provides better influence on durability. Magnetic treatment performed with higher number of cycles provides better wear resistance.

MODIFICATION OF WEAR TESTING MACHINE AND STUDY OF WEAR RESISTANCE

by
Ning Li

A Thesis
Submitted to the Faculty of
New Jersey Institute of Technology
in Partial Fulfillment of the Requirements for the Degree of
Master of Science in Mechanical Engineering

Department of Mechanical Engineering

January, 1993

APPROVAL PAGE

Modification of Wear Testing Machine
and
Study of Wear Resistance

Ning Li

Dr. Roman Dubrovsky, Thesis Adviser
Associate Professor of Mechanical Engineering, NJIT

Dr. R. Y. Chen, Committee Member
Professor of Mechanical Engineering, NJIT

Dr. A. Harnoy, Committee Member
Associate Professor of Mechanical Engineering, NJIT

BIOGRAPHICAL SKETCH

Author: Ning Li

Degree: Master of Science in Mechanical Engineering

Date: January, 1993

Undergraduate Education:

- Master of Science in Mechanical Engineering
  New Jersey Institute of Technology, Newark, NJ, 1993
- Bachelor of Science in Mechanical Engineering
  Shanghai University of Technology, Shanghai, China, 1986

Major: Mechanical Engineering

This thesis is dedicated to

my parents, Mr. Tao Li and Mrs. Fengzhen Chao

ACKNOWLEDGMENT

The author wishes to express her sincere gratitude to her thesis advisor, Dr. Roman Dubrovsky, for his guidance, both moral and financial support throughout this work.

Special thanks to Dr. R. Chen and Dr. A. Harnoy for serving as members of the committee.

Special appreciation extended to Mr. Karl Ulatowski and Mr. Don Rosander for their timely help and suggestions for setting up the new wear testing machine.

The author also like to express her thanks to the members of the Surface Engineering Laboratory, including: Mr. I-Tsong Shih, Mr. Wenge Yang, Mr. Nien-Sheng Lin, Mr. Tian-Zhong Xu for their valuable help and support.

The author's great thanks to her parents, who gave her the opportunity to study in the United States and gave her all the love and support to finish the work. Thank you both so much.

And finally, a thank you to all the people who helped me during my stay in the United States.

TABLE OF CONTENTS

Chapter **Page**

LIST OF TABLES

Table **Page**

LIST OF FIGURES

Figure **Page**

Figure **Page**

Figure **Page**

CHAPTER 1
INTRODUCTION

Wear is a popular phenomenon in our everyday life. Before the century, people already found that metal tools are stronger and harder to be worn than wood tools. And farmers found that bronze hoe is easier to wear off than iron one.

In the industry, wear of parts is one of the main reason for failure of parts. In United States only in 1985, it costs billions of Dollars for repairing parts due to wear. No surprises that enormous researches have been carried out on the wear. Unfortunately, there is no simple law of wear. On the whole, hard solids wear less than soft, although polyethylene wears less than steel. The wear generally increases with the distance rubbed and with the load applied when the other running conditions are remained same.

In order to lower the cost of the operation of the machinery. Lubricant has been introduced into wear system to reduce the friction, so that to reduce the wear of the contact surface. A lot of works also have been done on improving the wear resistance of machine components. Alloys, as well as different heat treatment processes, are used for better wear resistance. Surface treatments are widely used in these days because it raises the wear resistance of the surfaces and remains the core properties unchanged.

Wear testing is a very important step in the wear study. Various testing machines are developed for different wear testing methods and materials, as well as for different working conditions.

The shapes of the contact surfaces to be tested can be described as following:

1. Flat surface to flat surface
2. Curved surface to curved surface
3. Flat surface to curved surface

Since there are too many factors that can affect the running condition and lead to the wear results, particular testing machine should be used for certain test.

CHAPTER 2
BACKGROUND

2.1 Wear

Wear can be defined as the progressive loss of material from the operating surface of a body occurring as a result of relative motion at surface[1]. A potential wear situation exists whenever there is relative motion between two solids under load. Broadly speaking, the motion can be unidirectional or reciprocating either sliding or rolling. There may be a combination of rolling and sliding or wear may occur due to oscillatory movement at small amplitudes. In well-designed tribological systems, the removal of material is usually a very slow process, but it is very steady and continuous.

The wear behavior of a material is very complicated phenomenon in which various mechanisms and factors are involved. Several types of wear phenomenon occur, e.g., adhesive, abrasive, fatigue, corrosive, fretting, erosive wear by solid particles, fluid, and cavitation, which offer mean different things to different people depending on the emphasis intended. More over, definition of wear processes is imprecise and ambiguous. A wear classification scheme is needed to avoid ambiguity. In the literature, the classification of wear is based on the type of relative motion, as suggested by Siebel[2], and on the type of wear mechanism involved, as suggested by Burwell[3] and Bhushan[4].

2.1.1 Type of Wear

In the present discussion, emphasis is placed on the wear between solid surfaces. Depending on the nature of the movement or of the media involved in an interaction under load, the types of wear can be classified as follows.

1. Adhesive Wear

In this wear, the relative movement can be unidirectional or reciprocating sliding or interaction occurs under small amplitude oscillatory contact under load. The match surface peaks are known to flow plastically and to form strong work hardened junctions. As these breaks under an imposed tangential traction, material loss from the solids may occur.

2. Abrasive Wear

Abrasive particles in the form of wear debris or adventitious particles of grit and dust from the surrounding remain trapped at the sliding interface and remove material largely by ploughing.

3. Fatigue Wear

Fatigue wear is a result of cyclic loading. The repeating stresses in a rolling or sliding contact give rise to fatigue failure. The effects are mainly based on the action of stresses in or below the surfaces without meeting a direct physical contact of the surfaces under consideration.

4. Fretting Wear

Fretting is a form of wear which occurs as a result of oscillatory movement between two surfaces as in machine parts undergoing vibration.

5. Erosive Wear

Erosive wear results when grits impinge on solids while cavitation erosion may arise when a component rotates in a fluid medium.

2.1.2. Mechanism of Wear

1. Adhesive Wear

Adhesive wear processes are initiated by the interfacial adhesive junctions that form if solid materials are in contact on an atomic scale[5]. As a normal load is applied, local pressure at the asperities becomes extremely high. In some cases, the yield stress is exceeded, and the asperities deform plastically until the real area

of contact has increased sufficiently to support the applied load. In the absence of surface films, the surface would adhere together, but very small amounts of contaminant minimize or even prevent adhesion under purely normal loading[6]. However, relative tangential motion at the interface acts to disperse the contaminant films at the point of contact, and cold welding of the junctions can take place, Continued sliding causes the junctions to be sheared and new junctions to be formed. The chain of events that leads to the generation of wear particles includes the adhesion and fracture of the mating surface.

A small fragment of either surface becomes attached to the other surface. As sliding continues, this fragment constitutes a new asperity that becomes attached once more to the original surface. This transfer element is repeatedly passed from one surface to the other and grows quickly to a large size, absorbing many of the transfer elements so as to form a flakelike particle from materials of both rubbing elements[7]. Unstable thermal and dynamic conditions brought about by rapid growth of this transfer element finally account for its removal as a wear particle (Fig. 2.1).

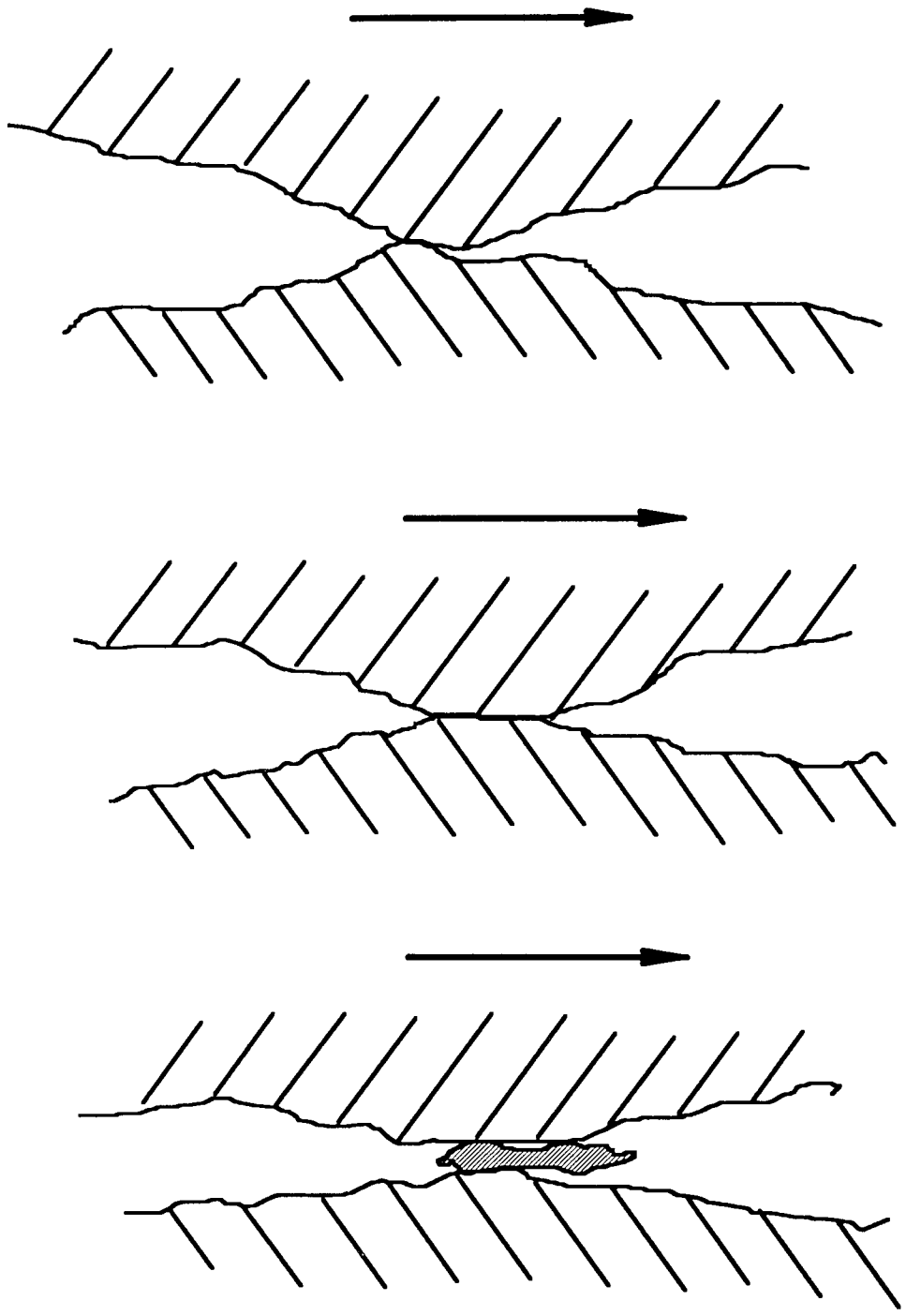

Fig. 2.1 Schematic of generation of wear particle as a result of adhesive wear process.

2. Abrasive Wear

Abrasive wear may be described as damage to a surface by a harder material. It is also sometimes called scratching, scoring, or gouging depending on the degree of severity. There are two general situations in which this type of wear occurs. In the first case, the hard surface is the harder if two rubbing surfaces (two-body abrasion), e.g., in mechanical operations such as grinding, cutting, and machining. In the second case, the hard surface is a third body, generally a small particle of grit or abrasive, caught between the two other surfaces and sufficiently harder than they are to abrade either one or both of them (three-body abrasion).

In the abrasive wear process, asperities of the harder surface press into the softer surface, with plastic flow of the softer surface occurring around the asperities from the harder surface. When a tangential notion is imposed, the harder surface removes the softer material by combined effects of microploughing, microcutting, and microcracking (Fig. 2.2)[8].

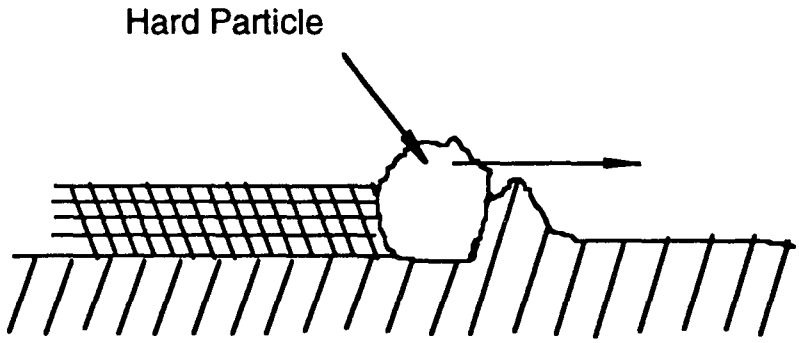

Fig. 2.2 Aspects of abrasive wear.

3. Fatigue Wear

Fatigue wear occurs on a rolling and/or sliding surface which experience continual application and release of hertzian stress. Since the shear stress is maximum some distance below the surface in a pure rolling contact (zero tangential stress at the surface), the failure initiates at the subsurface. If superimposed on the rolling contact there is also some sliding contact, then the location at which the shear stress is maximum, and therefore the position of failure, moves nearer to the surface. However, material are rarely perfect, and the exact position of ultimate failure will be influenced by inclusions, porosity, microcracks, and other facts (Fig. 2.3).

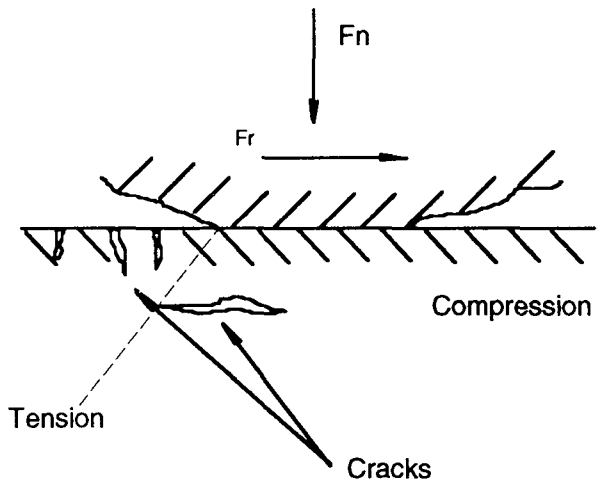

Fig. 2.3 Schematic of fatigue wear due to formation of surface and subsurface cracks.

4. Fretting Wear

Fretting wear takes place on the surface subjected to very small relative vibratory movement. It is initiated by adhesion, is amplified by corrosion, and has its main

effect by abrasion[9][10].

A typical example would be a splined out-of-line shaft coupling, in which the steel teeth undergo one small tangential movement per shaft revolution. As a result of the movement, adhering steel particles are produced (adhesive wear), and these oxidize (corrode) to Fe_2O_3. This is abrasive, and then causes abrasive wear if the surfaces.

2.2 Wear Resistance Testing

2.2.1 Methods of Wear Testing

There are several ways to do the test for different purposes. The test should simulate the actual working conditions as closest as possible. No single method can cover all the wear situation.

A general methodology is listed as follow. The four steps include determining a purpose, establishing a wear mode, defining a wear system, reporting a testing data.

At the start of any research project, it is highly beneficial to determine a purpose and corresponding objective. This step should not be overlooked or treated lightly. The direction taken in the wear test program will depend on the chosen purpose and objective. The purpose and objective can provide boundary conditions, operating conditions, and material selection criteria for the test program. A typical purpose might be to develop wear preventative material treatments or coatings, while the objective might be to provide guidelines for the application of the treatments and coatings to give optimal wear resistance.

After the purpose and objective of the test have been decided upon, it is necessary to establish a wear mode discussed previously. A decision must be made regarding which wear mode, or combined modes, is likely to dominate the

wear system. For example, adhesion is the predominant wear mode displayed by damaged bushings, cams, and bearings.

The third step is to define the wear system. It was mentioned earlier that wear should be treated as a system response of a material rather than a material property.

The next step is the treatment and reporting of test. Regardless of the apparatus chosen to perform the test, all elements in the wear system should be listed out. The entire operating variables, tribosystem structure, and tribological characteristics should be recorded. The operating variables are the mechanical work inputs to the wear system. Tribosystem structure gives a complete description of the test materials, test surface, and test environment. Tribological characteristics are the results of the wear test. A correctly designed data sheet is useful which not only monitors the elements, but also serves as a wear test checklist. Not all the wear tests have the same data sheet. But the major concern is that all elements having an effect on the wear system be observed and recorded.

2.2.2. Wear Testing Devices

After deciding upon a suitable methodology for testing the wear system of interest, attention must be turned toward the selection of an appropriate wear testing apparatus. An entire range of standardized testing machinery has been designed and produced, each capable of reproducing a particular wear mode. The sheer number of testing device available for each wear made prohibits a complete listing. However, some common metal on metal wear tests are block-on-roller, roller-on-flat, pin-on-disk, sphere-on-flat, pin-on-flat, roller-on-roller, cross cylinders, pin-on-cylinder (Fig. 2.4). The important point to remember when selecting a wear test is to make sure that the test environment is the most similar to the actual working condition.

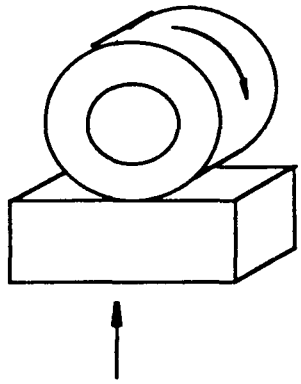

Block-on-Roller

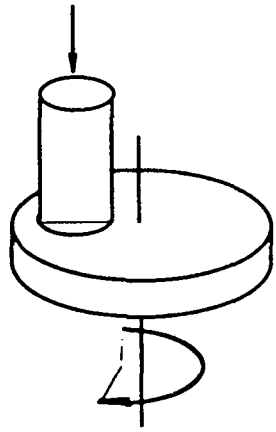

Pin-on-Disk

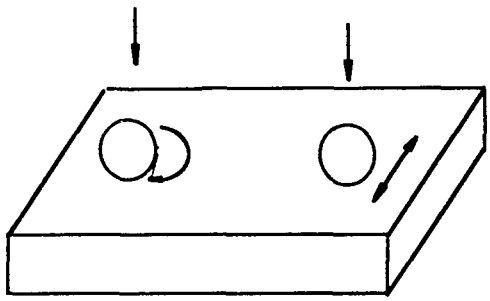

Sphere-on-Flat

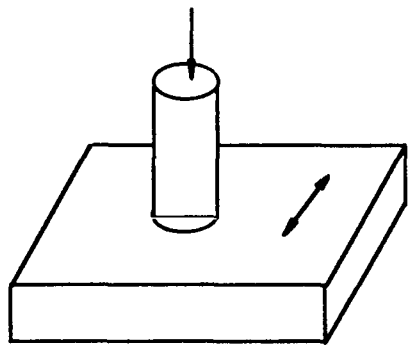

Pin-on-Flat

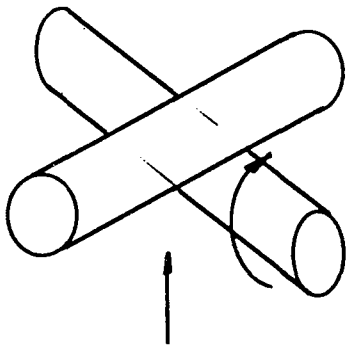

Cross Cylinder

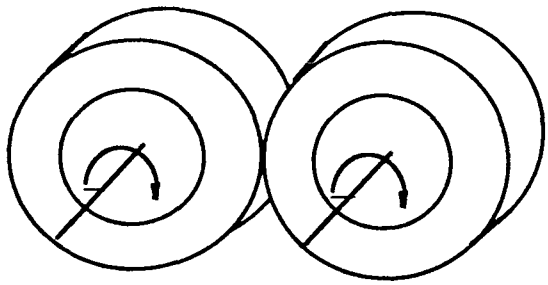

Roller-on-Roller

Fig. 2.4 Common methods of wear testing.

2.3 Advantages and Disadvantages of Existing Testing Machine

A roller-on-block wear testing machine has been used to carry out all the wear test data for the discussion in next few chapters.

2.3.1. Advantages

The existing test machine was designed and improved by the student of the Surface Engineering Laboratory of Mechanical Engineering Department at New Jersey Institute of Technology[11]. It provides laboratory test for determining the wear resistance of material under sliding wear. It can rank pairs of materials according to their sliding wear characteristics under various conditions.

The machine provides a rotation on a roller and keep the block in stable condition. A strain gauge is connected to a personal computer to record the moment of the shaft, which will be used to carry out the friction moment of the test material. A preprogrammed controller is used to control the start and stop of the motor automatically.

An important attribute of this test is that it is very flexible, any material can be used to, blocks and rollers can be tested. Thus potential materials combinations are endless. In addition, the test can be run with various lubricants, liquids, or gaseous atmospheres, as desired, to simulate the service conditions. Load can also be adjusted to better correspond to service requirements.

2.3.2. Disadvantages

Block-on-roller practice can only prescribe the test procedure and method of calculating and reporting data. The choice of test operating parameters is left to the user, with the exception that sliding distance is specified because wear usually has no linear relationship with sliding distance in this test. Selected combination

of tested pair (block-roller) provides only sliding speed in maximum range and not able to perform a wear test at variable sliding speeds.

2.4 Goal and Objectives

The goal of this work is to modify an existing wear testing machine designed on roller to roller principle and perform a wear resistant test for selected specimens.

To reach this goal a new load mechanism should be designed, bearing supporting suspended gearbox and frame should be redesigned, pushing mechanism should be corrected, all set up should realigned on a machined table. Additional objective of this work is to perform a stress analysis for designed frame of loading mechanism as well as define wear resistance for specimens treated differently by plasma ion nitriding and magnetic field.

CHAPTER 3

METHODOLOGY OF WEAR TESTING

3.1 Wear Resistance

Wear is a complicated phenomenon, because there are so many elements involved in. Any change on any of the elements may cause change of wear.

During study on the wear behavior of materials which performed by the great genius Leonardo da Vinci, people found that wear increases with load and that the direction of wear follows the main vector of the load.

Friction force plays a very important role on wear. Almost 9,000 years ago people discovered a friction force, and started to use it and overcome it. The first practical application seems to be the use of friction heat in lighting a fire. The ancient Egyptians were already using liquid lubricant in order to minimized the work required to transport heavy objects.

Apparently reducing of friction force can decrease the wear rate of object. Wear occurs between two contact surfaces under relative motion. Lubricant is used to separate the contact surfaces, and it generates a fluid film which can easily be sheared without causing any damage to the surface.

Material properties and surface roughness also will effect the wear. As we know, the higher hardness of material can prevent some abrasive wear, but brittle surface will easily produce a fatigue wear.

Studies in tribology have found that roughness of surface influences the wear rate.

3.1.1 Parameters of Wear Resistance

Wear arising from mechanism of adhesion, abrasion and delamation has been found proportional to the applied normal load and sliding distance. In the case of

abrasion and for some materials under adhesion and delamination wear mechanisms, an inverse relation has been found between wear and hardness of the wear surface, i.e.,

$$W = k\frac{N \cdot S}{C \cdot H} \tag{3.1}$$

where, W=Worn Volume;

N=Normal Load;

S=Sliding Distance;

H=Hardness;

k=Wear Constant.

C=Geometrical constant, equal 1 for abrasion wear and equal 3 for adhesion wear.

Since both hardness and wear constant depend on the microstructure of materials, they should not appear independently in the equation. Therefore the wear equation can be written as:

$$W = k \cdot N \cdot S \tag{3.2}$$

where, k=wear factor. Although both equations (3.1) and (3.2) can be derived by considering the basic mechanisms of abrasion, adhesion or delamination, the constant must be determined experimentally[13].

The only work which has revealed any systematic wear behavior, had been carried out under conditions often far removed from conditions existing in any particular wear system. For this reason, no description of laws of wear has been so widely accepted as the law of friction.

The experiment has been done in this work is try to find out the effect of Plasma ion-nitriding treatment and magnetic treatment on wear resistance of alloy steel.

3.1.2 General Description of Existing Wear Testing Machine

The wear testing machine used in this work, as mentioned in previous chapter, is a block-on-roller machine.

A one horse power, 1750 rpm, three phases induce motor is suspended by two parallel shafts resting on two pillow block bearings. One shaft is connected to a mechanical counter which is capable of recording number of revolution, another shaft is coupled to a parallel shaft gear reducer with a reduction ratio of 6.3:1. The output shaft of the gear reducer is directly coupled to the shaft where the test roller is mounted. The test shoe is fixed in a shoe holder right below the roller. The loading mechanism is hooked up on the shoe holder through a linear bearing which provides the vertical motion of the holder to keep the contact between two testing parts.

The loading mechanism includes levers, cam, follower, and a DC motor as a cam driver. The load is amplifered through the lever by 1:72.

The base of the suspended motor is attached to an arm which supported by a rod. A steel frame is mounted on the other side of the motor to keep balance. A strain gauge is mounted on the arm to pick up the deflection in order to carry out the moment at the motor. Further discussion will be provided in next section.

3.1.3 Pressure

When two surfaces are brought to contact the deformation of the contact surface is either in an elastic or plastic manner. The plastic deformation is always the point which is considered. With plastic deformation the stress-strain relationship is

more complex because some deformation persists even after removal of the load. In sliding wear the deformation is accumulated along the surface and plastic deformation is reached easily thereby resulting in damaged surfaces. This also is the reason that the contact stresses are important to the surface failure.

In studying the elastic-plastic stress field in the subsurface regions of sliding asperity contacts and the possible dislocation interaction, Suh has suggested the following details of the events leading to subsurface failure. They thought that the subsurface stresses cause the localized inelastic deformation in the material (yielding or distortion). These inelastic deformations initiate the crack, propagate the crack, and finally form the wear particle. So, from the distribution of surface stresses people can indicate the place where the crack may start and the direction of crack propagation.

The contact area of block-on-roller test apparatus varies during the test. The initial contact area is a line that can lead to Hertzian stresses expressed by Equation (3.3).

$$\sigma_{max} = .798\sqrt{\frac{W}{tD[\frac{1-\upsilon_1^2}{E_1}+\frac{1-\upsilon_1^2}{E_2}]}} \tag{3.3}$$

for non-self mating wear surface

$$\sigma_{max} = 0.564\sqrt{\frac{WE_1}{tD(1-\upsilon_1^2)}} \tag{3.4}$$

for self-mating wear test or for materials with same plastic constants.

where, σ=mean compressive stresses, MPa (psi),

W=normal load, N (lbf);

t=block width, mm (in");

υ_1=Possion's ratio for block material;

υ_2=Possion's ratio for roller material;

E_1=elastic modulus for block material, MPa (psi), and

E_2=elastic modulus for roller material, MPa (psi).

3.1.4 Sliding Distance

During the whole test period, the applied load is kept same, and the motor provides a constant output which is 1750 rpm.

The revolution of roller can be gotten:

$$R_r = R_m \times r \tag{3.5}$$

where, R_m=revolution per minute of motor;

R_r=revolution per minute of roller;

r=ratio of gear reducer.

The sliding distance of roller every minute is:

$$D = R_r \cdot \pi \cdot d \tag{3.6}$$

where, D=distance roller traveled;

d=diameter of roller.

Since the number of revolution per minute of the roller is a constant, therefore in this test, the wear rate, which is defined as volume of material to be removed in unit distance of sliding, also can be defined as a function of time.

The results of this work, in later discussion, will be stated in terms of time instead of sliding distance .

3.2. Wear Testing

3.2.1 Measurement of Friction Coefficient

A strain gauge is mounted on the arm attached to the motor. When it turned on, the arm deflects, and the strain gauge picks up the signal. The analog signals are transferred to a personal computer through an A/D convert board (Dascon-1, Metra Byte Co.). The output signals are recorded onto disk in a time interval from second to minutes upon previous setting.

Friction moment and friction force can be carried out by further data processing. Several equations are developed for this calculation.

$$P_f = P_m \cdot \eta \tag{3.7}$$

$$P_f = \frac{T_f \cdot N_r}{63000} \tag{3.8}$$

$$P_m = \frac{M_m \cdot N}{63000} \tag{3.9}$$

where, P_m = motor output;

η = system efficiency;

T_f = torque generated by friction force;

N_r = rotation of roller per minute;

N = rotation of motor per minute;

M_m= moment at motor,

$$T_f = F_f \cdot r \tag{3.10}$$

$$F_f = f \cdot W \tag{3.11}$$

where, W = Load (normal);

f = friction coefficient,

From the energy equilibrium,

$$\frac{T_f \cdot N_r}{63000} = \frac{M_m \cdot N}{63000} \cdot \eta \tag{3.12}$$

$$F_f \cdot r \cdot N_r = M_m \cdot N \cdot \eta \tag{3.13}$$

$$f = \frac{N}{N_r} \cdot \frac{\eta}{r} \cdot \frac{1}{W} M_m \tag{3.14}$$

Since revolution of motor and roller, N and N_r are known, and the efficiency of the system, the radius of roller and the normal load applied are constant. The equation (3.14) can be written as:

$$f = k \cdot M_m \tag{3.15}$$

where, $k = \frac{N}{N_r} \cdot \frac{\eta}{r} \cdot \frac{1}{W}$.

3.2.2 Surface Roughness Measurement

A profile measuring system is employed to measure the surface roughness before and after every test interval. As shown in Fig 3.2, the system is composed of three major units[14]:

1. Daedal moving table control unit;
2. Surfanalizer-40000 unit;
3. Dell computer unit.

The probe of the profile meter can travel along the X direction to obtain a profile. After one cycle the probe returns to the starting point and displaces at the the Y direction to measure the second profile if multi-profile measurement

required. By this way it can scan the whole test surface.

While the probe measures a profile on the work piece, the obtained signal is amplified and then sent to a microprocessor where A/D conversion, digital filter and some signal treatment are done. The data is then transmitted to an IBM personal computer for data analysis and stored in data files.

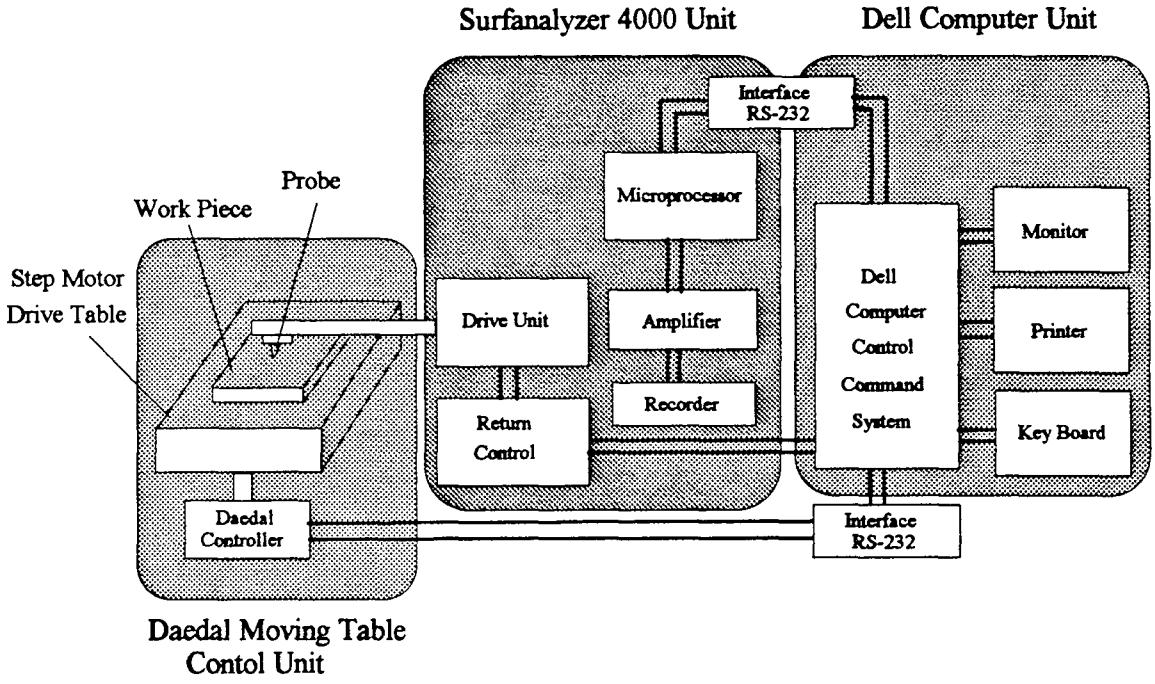

Fig. 3.1 Surface roughness measuring system.

In order to obtain accurate results, some procedures are carefully followed:

1. To ensure that stylus follows exactly the contour of the surface being measured, a force is needed to push it against the surface. Values of stylus force have been specified which will enable roughness measurement to be made accurately on materials.
2. During the testing, a sufficient length of surface must be traversed to ensure that the full reading characteristic of the surface is obtained.

Besides, the first 400 sample points are deleted from the record to ensure the accuracy of the result.

3. Because the worn surface is a random surface, so each time 3 profiles cross the scar are measured for adequate measurements.

Test setups are as follows:

- Cutoff = 0.8 mm;
- Drive speed = 0.25 mm/s;
- travel length = 6 mm;
- Sampling points of whole length = 6000;
- Motor steps = 10,000/rev;
- Linear motion table resolution: 5μm.

Roughness average R_a, root-mean-square (rms) roughness R_q, ten-point height R_Z, and maximum peak-to-valley roughness height are calculated for every profile.

3.2.3 Wear Measurement

Wear debris can be measured either as a weight loss or a change in volume, or a change of dimensions for one or both sliding members. The following 6 wear criteria have been proposed and used [15].

1. Linear wear rate

$$K_L = \frac{\text{Thickness of layer removed}}{\text{Sliding distance}} = \frac{h}{L};$$

2. Volumetric wear rate

$$K_v = \frac{\text{Volume of layer removed}}{\text{Sliding distance} \times \text{apparent area}} = \frac{\Delta V}{LA_a};$$

3. Energetic wear rate

$$K_E = \frac{\text{Volume of layer removed}}{\text{Work of friction}} = \frac{\Delta V}{FL};$$

4. Gravimetric wear rate

$$K_w = \frac{\text{Weight of layer removed}}{\text{Sliding distance} \times \text{Apparent area}} = \frac{\Delta W}{LA_a};$$

5. Abradibility

$$\gamma = \frac{\text{Volume abraded}}{\text{Work of friction}} = \frac{\Delta V}{FL} = \frac{\Delta V}{fWL} = \frac{\Delta V / WL}{fWL} = \frac{A'}{f};$$

6. Coefficient of abrasion resistance

$$\gamma = \frac{\text{Work of friction}}{\text{Volume abraded}} = \frac{1}{\gamma} = \frac{1}{K_E} = \frac{f}{A'};$$

where, L=sliding distance

F=friction force;

f=coefficient of sliding friction;

A'=abrasion factor.

In this work, wear rate is expressed by weigh loss per minute, which is the easiest method of measuring wear rate. To carry out a weighing, it is necessary to remove from the sliding mechanism the component to be examined, to clean it carefully. In the test an ultrasonic cleaner is used with Leco multi-purpose clean solvent to clean the test object--shoe and roller. After 10 minutes vibrating in the cleaner, the test objects are wiped by a soft tissue with acetone. Then put on an

electrical balance with resolution of 10^{-5}gm.

The limit of resolution of the weighing method is generally around 10^{-4}gm. It is set by three factors, namely: our inability to clean materials consistently enough, so that the residues left on them produces a weight uncertainty; the material transfer, unpredictable in direction, which occurs at the points where our component is fastened into the sliding mechanism; lastly by the limit of resolution of the typical chemical balance used for wear measurements.

CHAPTER 4

LOAD MECHANISM DESIGN

4.1 Load Mechanism Design History and Problems

The new roller-on-roller wear testing machine was designed by students of Surface Engineering Laboratory of Mechanical Engineering Department during 1989-1991 under supervision of Dr. Roman Dubrovsky. The wear test machine as shown in Fig. 4.1, consists of a one horse power DC motor, a gearbox I (6.2:1) which will hold one testing roller, a shaft assembly holding another test roller, a stationary gearbox II (6.2:1), an AC motor, levers, and a linear bearing set.

When the load is applied the force is amplified through the levers and pushes up the linear bearing along with the pusher (see Fig. 4.1 a), then the pusher pushes the converter attached on gearbox I, causing the gearbox assembly turns around the lower shaft till the two rollers contact each other. The rollers will keep in contact until the load is taken off.

The DC motor, through gearbox I, drives the roller I at a preselected direction and speed, while the AC motor drives the shaft assembly and roller through gearbox II at a fixed speed and direction. By selecting different speed and direction of the DC motor, the two rollers can have several sliding speeds. This enlarges the testing capability of the test machine.

The steel working table, levers, linear bearing and shaft assembly are manufactured and assembled before the author started this work.

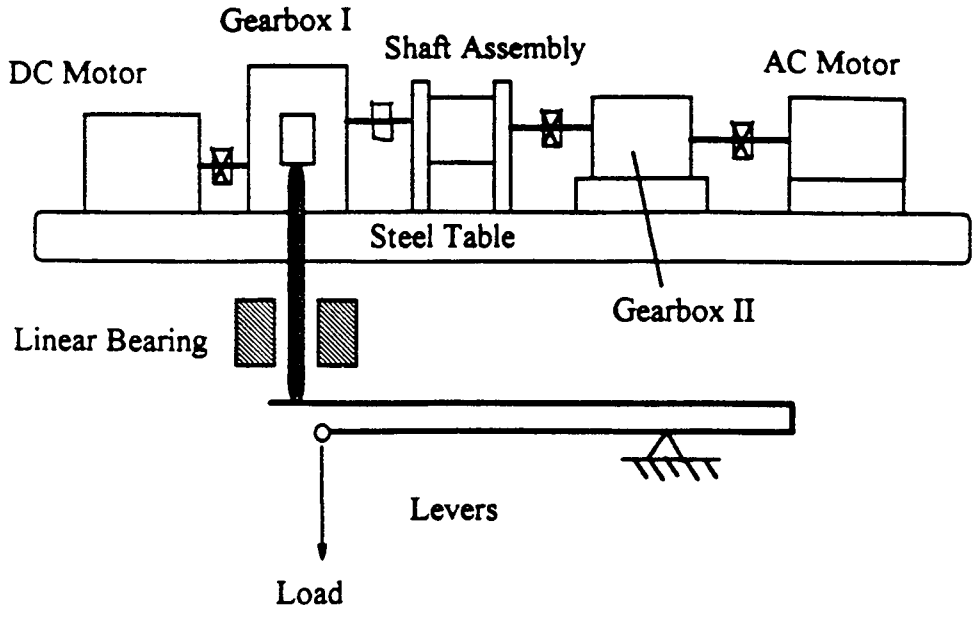

(a)

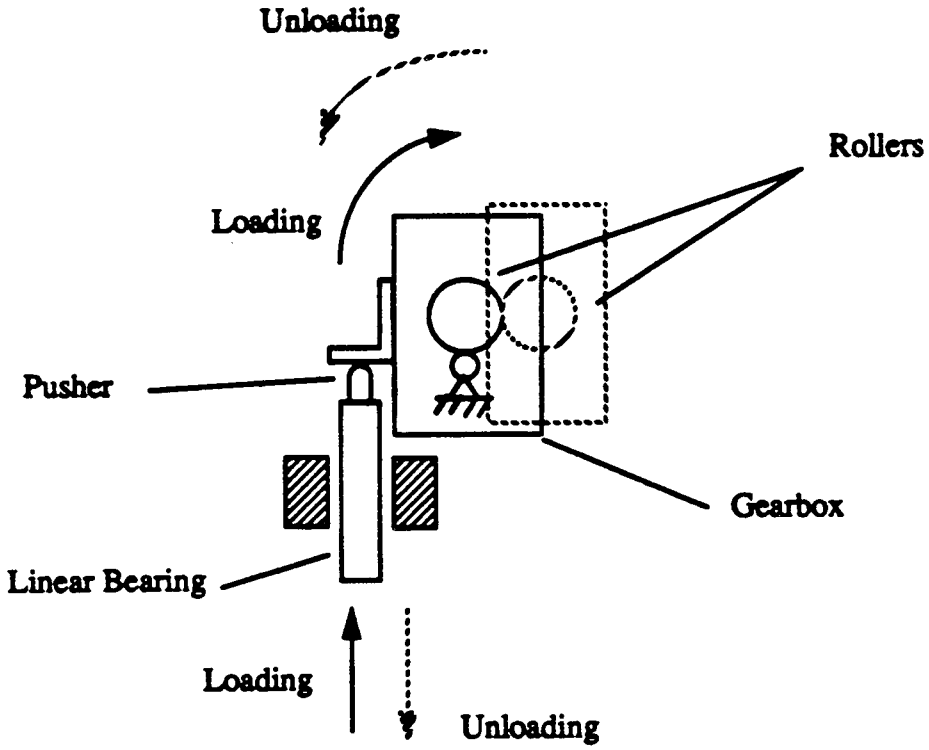

(b)

Fig. 4.1 Original layout of roller-on-roller wear testing machine

Because the gearbox I in initial design is no longer available, a City Hub parallel shaft drives model 240 (6.2:1) gearbox was selected in 1990 to replace the initial one. The input shaft of this gearbox was redesigned in order to suspend the gearbox by two bearings on each side[16] (Fig. 4.2).

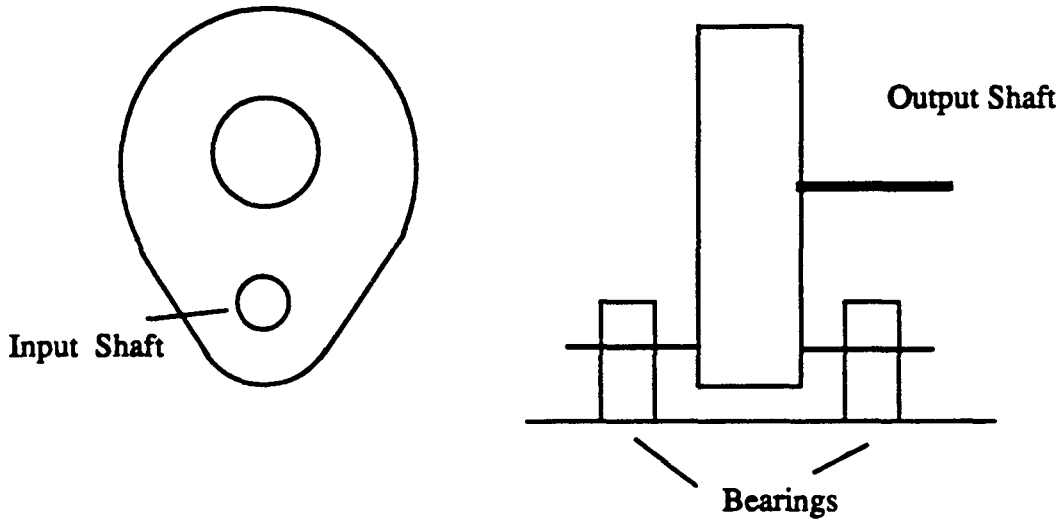

Fig. 4.2 City Hub parallel drive gearbox.

Since the change of the gearbox the conjunctive parts have to be redesigned, as well as the elevation of the other components has to be readjusted. This work is started on the base of existing parts and assemblies. The loading mechanism is redesigned and manufactured as well as other parts such as bearing base, etc. A GSE model 5353 load cell is put in the load mechanism to pick up loading information during the test.

4.2 Description of Load Mechanism

In order to transfer the vertical motion of the sliding pusher attached on the linear bearing into a horizontal motion of the roller I which is mounted on the output shaft of the gearbox I, a special frame set is designed to hold the suspended gearbox I and to provide a linkage from the gearbox to the pusher (Fig. 4.3).

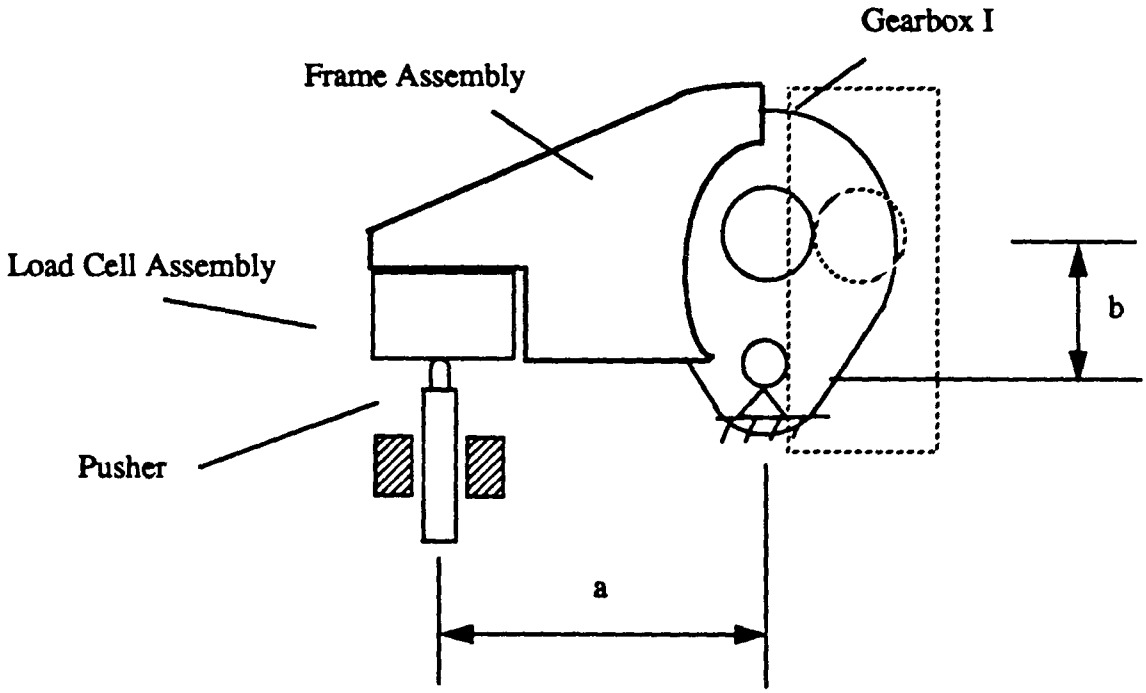

Fig. 4.3 Gearbox I and load mechanism.

A CSG Model 5353 load cell needs to be introduced into the loading mechanism to pick up the loading information during the testing. The best location for the load cell in the loading assembly is between the pusher and frame where the load cell is under pure compression when the load is applied.

The final load applied on the roller can be calculated from the read out of the load cell by:

$$\text{Load on Roller} = \text{Load Cell Read Out} \times \frac{b}{a}$$

where, a = perpendicular distance from pivot to the load applied on load cell.

b = distance from roller to pivot.

A large working space is needed to take out the rollers after the test, especially while the rollers are at very high temperature after the test. However there is not enough room between end of the output shaft of gearbox I and frame of the shaft assembly to take out the test roller. The gearbox has to swing out (turn counter clockwise in Fig. 4.3), so that the roller can be taken out without the shaft assembly blocking on the way. But in order to keep the accuracy of load transfer only very small travel distance is allowed for the levers along with the pusher. So even when the machine is unloaded, the pusher will travel down little bit which is still not enough for the gearbox to swing down. The only solution is to take some part out to make room for the gearbox to swing out when it is unloaded. The load cell assembly is such a part ideal to be taken out for this purpose.

4.2.1 Gearbox Frame Design

The frame assembly provides the linkage between the gearbox and the pushing up mechanism. It transfers the huge load from the pusher to the roller. It should be very durable. Meanwhile it will swing with the gearbox during the loading and unloading period. It should be simple and not too heavy.

Shown in Fig. 4.4, two specially designed 1/4" thick plates (part 1 & 2) are assembled on two sides of the gearbox. Two small side plates (part 5) are inserted between the gearbox and large plates to provide the rigidity of the whole assembly.

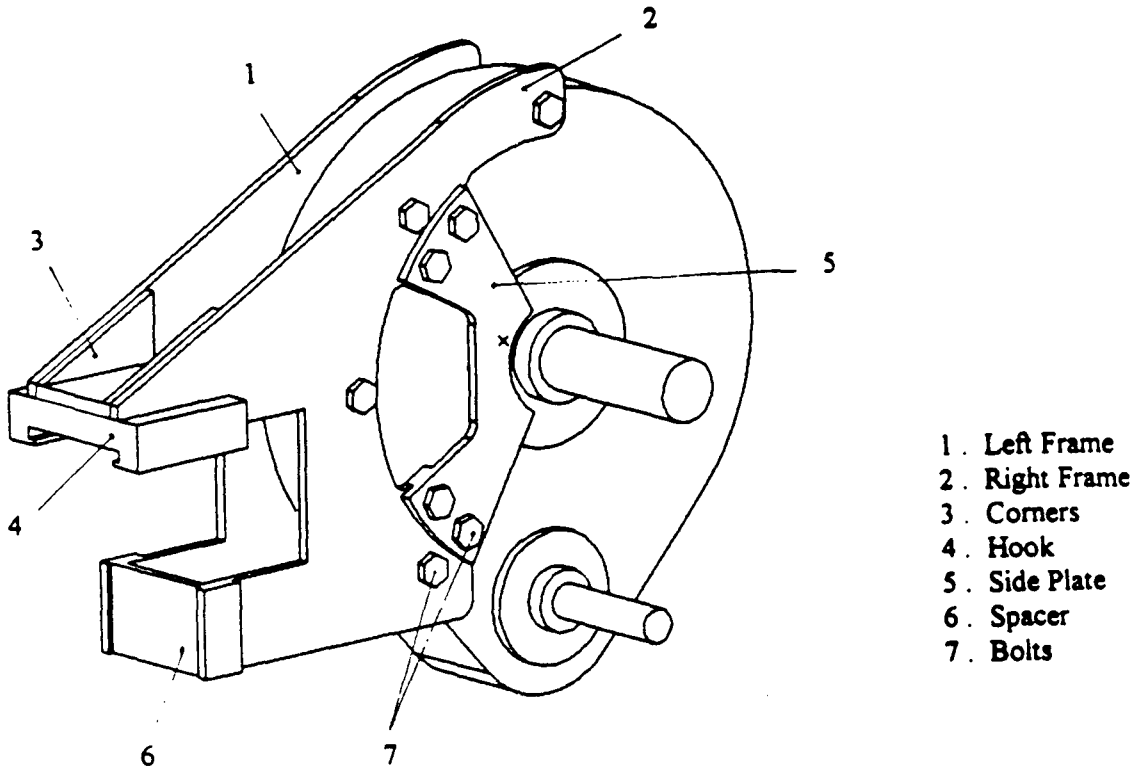

Fig. 4.4 Gearbox frame assembly.

These four parts are mounted on the gearbox through existing bolts on the gearbox. Two corners are used to link the plates and the Hook which provides a T shape slot for the load cell assembly to slide in. Spacer and dividers are specially designed to make the frame assembly more durable. The spacer also work as a stop while the load cell assembly slides in.

4.2.2 Design of Load Cell Assembly

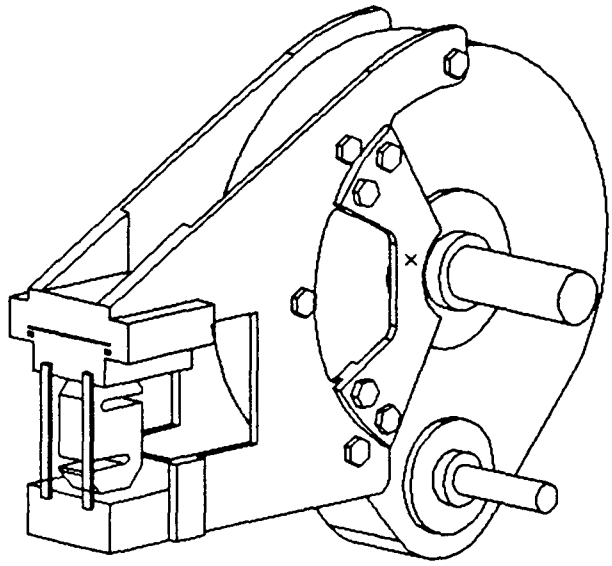

Fig. 4.5 Load cell and frame assembly.

A CGS Model 5353 load cell will be used in the loading system to pick up loading information. A load cell house is needed to hold the load cell and inserts into the frame assembly of the loading mechanism (Fig. 4.5). As shown in Fig. 4.6, two plates (part 2 & 5) are bolted on through two 1/2" bolt holes on top and bottom of the load cell. In order to make an even load distribution, another top plate with two lips (part 1) designed to connect the part 2. And the lips are designed to match the "T" groove on the frame assembly for sliding the whole load cell assembly into the Hook of the frame assembly. Another bottom plate (part 6) is employed to block the bolt hole on part 5, enabling a firm connection between the pusher and the load cell assembly. Handles (part 3) are designed for easy sliding in and taking out of the load cell assembly during the loading and unloading period. While the load cell

assembly slides into the Hook of the frame assembly, it will be stopped by the spacer (part 6 in Fig. 4.4), as soon as it reaches the working position.

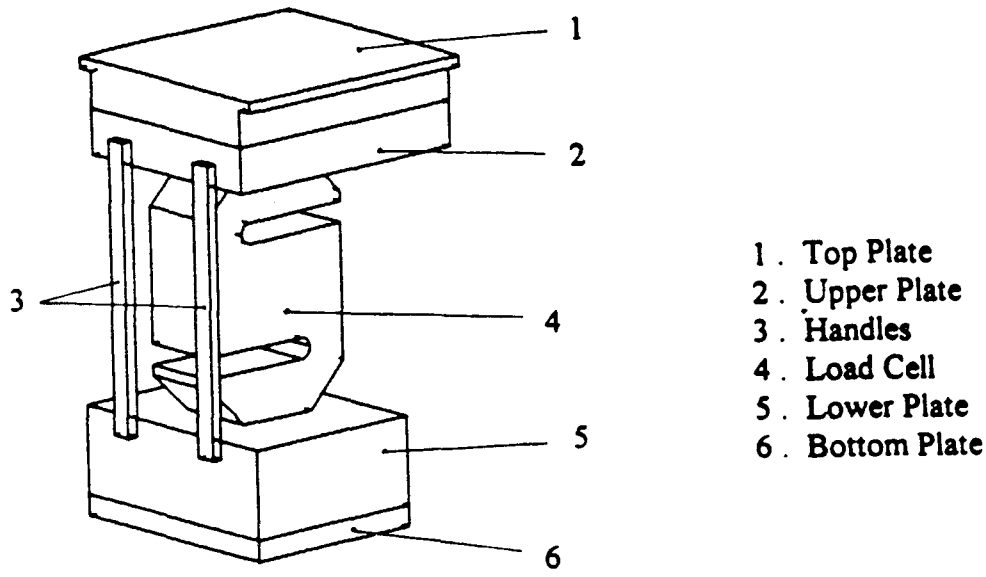

Fig. 4.6 Load cell assembly.

4.2.3 Design of Special Pillow Block Bearing Base

The gearbox I was originally supported by a pair of block bearing. Since the design load of the system is 1,500 lb., the bearing will sustain huge load, and the cast-iron pillow block bearings obviously will not be capable of handling such large load. A pair of special heavy duty pillow block bearing bases are designed and made from AISI 4030 steel to replace the original one (Fig. 4.7). The new bearing base was also designed to put in account required gearbox shaft alignment with the output shaft of the DC motor. Selected new gearbox requires that the originally made parts have to be elevated for lining up.

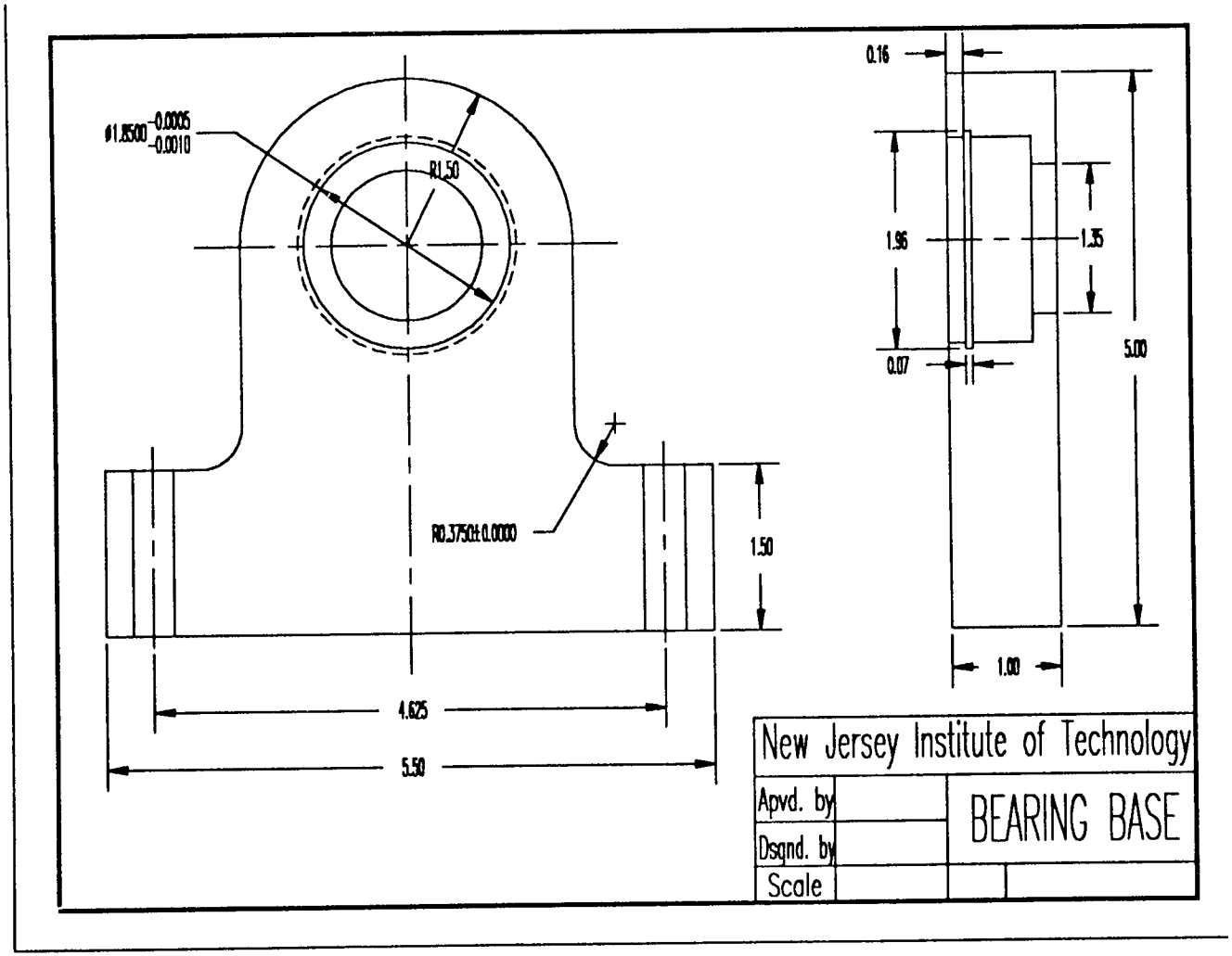

Fig. 4.7 Bearing Base

4.2.4. Correction and Adjustment of Pushing Mechanism

As shown in Fig. 4.1, the pushing mechanism includes levers, a linear bearing and a pusher on top of linear bearing. The originally installed linear bearing is too high to serve the newly designed loading mechanism. It was necessary to adjust it and incorporate it into new dimensional chain. Because the top of the pusher will sustain a very high contact stresses, the existing pusher with a slot on the top (Fig. 4.8a) should be redesigned as shown in Fig. 4.8b to provide permanent contact and self alignment.

(a) Original pusher (b) Redesigned pusher

Fig. 4.8 Pusher

4.3 Stress Analysis

Looking over the unit among all parts, only two plates are under tension stresses. Because the yield compression stresses are much larger than the tension stresses, the stress analysis should be only done for most critically loaded parts. In this case, it should be done on the plates. Because of the symmetrical structure, only one large plate needs to be analyzed.

Due to the complex shape of the frame structure the finite element method is used for the stress analysis.

4.3.1 Finite Element Stress Analysis Procedures

Steps involved in the finite element analysis of a typical problem are listed as follows[17].

1. Discretization (or representation) of the given domain into a collection of preselected finite elements. (This step can be postponed until after the finite-element formulation of the equation is completed.)
   a. Construct the finite element mesh of preselected elements.
   b. Number the nodes and elements.
   c. Generate the geometric properties (e.g., coordinates, cross-sectional areas, etc.) needed for the problem.
2. Derivation of element equations for all typical elements in the mesh.
   a. Construct the variational formulation of the given differential equation over the typical element.
   b. Assume that a typical dependent variable u is of the form

$$u = \sum_{i=1}^{n} u_i \psi_i$$

   and substitute it into step 2a to obtain element equations in the form

$$[K^{(e)}]\{u^{(e)}\} = \{F^{(e)}\}$$

   c. Derive or select, if already available in the literature, element interpolation functions ψ_i and compute the element matrices.
3. Assembly of element equation to obtain the equations of the whole problem.
   a. Identify the interelement continuity conditions among the primary variables (relationship between the local degrees of freedom and the global degrees

of freedom -- connectivity of elements) by relation element nodes to global nodes.

b. Identify the "equilibrium" conditions among the secondary variables (relationship between the local source or force components and the globally specified source components).

c. Assemble element equations using steps 3a and 3b superposition property.

4. Imposition of the boundary conditions of the problem.
   a. Identify the specified global primary degrees of freedom.
   b. Identify the specified global secondary degrees of freedom (if not already done in step 3b).
5. Solution of the assembled equations.
6. Post processing of the results.
   a. Compute the gradient of the solution or other desired quantities from the primary degrees of freedom computed on step 5.
   b. Represent the results in tabular and /or graphic form.

4.3.2 Plane Stress Analysis

Consider a linear elastic solid Ω of uniform thickness h (say, in the z direction) bounded by two parallel planes (say, by planes z = -h/2 and z = h/2) and by any closed boundary Γ. If the thickness is small compared with the lateral dimensions (x,y in this case), the problem is considered to be a plane stress problem. Plane stress problem is simplification of three-dimensional elasticity problem under the following assumptions on loading: the body forces, if any exist, cannot vary in the direction of the body thickness and cannot have components in the z direction; the applied boundary forces cannot have components in the z direction and must be uniformly distributed across the thickness (i.e., constant in the z direction); and no loads can be applied on the parallel planes bounding the top and bottom surfaces.

The assumption that the stresses are zero on the parallel planes implies that for plane stress problems (body is very thin) the stresses in the z direction are negligibly small. And the strains in the z direction are zero.

The Equilibrium Equation of a plane Ω in terms of stresses is

$$\left.\begin{aligned}\frac{\partial \sigma_x}{\partial x}+\frac{\partial \tau_{xy}}{\partial y}+f_x=0\\ \frac{\partial \tau_{xy}}{\partial x}+\frac{\partial \sigma y}{\partial y}+f_y=0\end{aligned}\right\} \text{ in } \Omega. \tag{4.1}$$

Where f_x and f_y denote the body forces along the x and y directions.

The stress -strain relations are

$$\begin{aligned}\sigma_x &= C_{11}\varepsilon_x + C_{12}\varepsilon_y\\ \sigma_y &= C_{12}\varepsilon_x + C_{22}\varepsilon_y\\ \tau_{xy} &= C_{33}\gamma_{xy}\end{aligned} \tag{4.2}$$

where, $C_{ij}(C_{ij}=C_{ji})$ are the elastic (material) constants. For an isotropic elastic body, they ate given in terms of the modulus of elasticity E and Poison's ratio ν by

$$C_{11}=C_{21}=\frac{E}{1-\nu^2}\ ,\ C_{12}=\frac{\nu E}{1-\nu^2}\ ,\ C_{33}=\frac{E}{2(1+\nu)} \tag{4.2a}$$

The strain-displacement relations are:

$$\varepsilon_x=\frac{\partial u}{\partial x}\ ,\quad \varepsilon_y=\frac{\partial v}{\partial y}\ ,\quad \gamma_{xy}=\frac{\partial u}{\partial y}+\frac{\partial v}{\partial x} \tag{4.3}$$

The boundary conditions

Body force

$$\left.\begin{aligned}\sigma_x n_x + \tau_{xy} n_y &= \hat{t}_x \\ \tau_{xy} n_x + \sigma_y n_y &= \hat{t}_y\end{aligned}\right\} \quad \text{on } \Gamma_1 \tag{4.4}$$

Displacement

$$\left.\begin{aligned}u &= \hat{u} \\ v &= \hat{v}\end{aligned}\right\} \text{on } \Gamma_2 \tag{4.5}$$

where $\hat{n} = (n_x, n_y)$ denotes the unit normal to the boundary Γ, Γ_1 and Γ_2 are (disjoint) portions of the boundary (Γ_1 and Γ_2 do not overlap except for a small number if discrete points -- singular points), $\hat{t}_x$ and $\hat{t}_y$ denote specified boundary (traction) forces, $\hat{u}$ and $\hat{v}$ are specified displacements, and h is the thickness of the plate.

Substitute Equations (4.3) into Eqs. (4.2), then Eqs. (4.2) into (4.1), we can get

$$\left.\begin{aligned}-\frac{\partial}{\partial x}(C_{11}\frac{\partial u}{\partial x} + C_{12}\frac{\partial v}{\partial y}) - C_{33}\frac{\partial}{\partial y}(\frac{\partial u}{\partial y} + \frac{\partial v}{\partial x}) &= f_x \\ -C_{33}\frac{\partial}{\partial x}(\frac{\partial u}{\partial y} + \frac{\partial v}{\partial x}) - \frac{\partial}{\partial y}(C_{12}\frac{\partial u}{\partial x} + C_{22}\frac{\partial v}{\partial y}) &= f_y\end{aligned}\right\} \quad \text{in } \Omega \tag{4.6}$$

And Eqs(4.4), can be written as,

$$\left.\begin{aligned}t_x \equiv (C_{11}\frac{\partial u}{\partial x} + C_{12}\frac{\partial v}{\partial y})n_x - C_{33}(\frac{\partial u}{\partial y} + \frac{\partial v}{\partial x})n_y &= \hat{t}_x \\ t_y \equiv C_{33}(\frac{\partial u}{\partial y} + \frac{\partial v}{\partial x})n_x - (C_{12}\frac{\partial u}{\partial x} + C_{22}\frac{\partial v}{\partial y})n_y &= \hat{t}_y\end{aligned}\right\} \text{ on } \Gamma_1 \tag{4.7}$$

The variational form of Eqs. (4.4) over an element Ω^e is given by multiplying the first equation with a test function w_1 and the second one with a test function w_2 and integrating the results by parts [to trade the second differential to w_i , (i = 1, 2)]. We have

$$
\begin{aligned}
0 &= \int_{\Omega^e} \{\frac{\partial w_1}{\partial x}(C_{11}\frac{\partial u}{\partial x}+C_{12}\frac{\partial v}{\partial y})+C_{33}\frac{\partial w_1}{\partial y}(\frac{\partial u}{\partial y}+\frac{\partial v}{\partial x})-w_1 f_x\}dxdy-\oint_{\Gamma^e} w_1 t_x ds \\
0 &= \int_{\Omega^e} \{C_{33}\frac{\partial w_2}{\partial x}(\frac{\partial u}{\partial y}+\frac{\partial v}{\partial x})+\frac{\partial w_2}{\partial y}(C_{12}\frac{\partial u}{\partial x}+C_{22}\frac{\partial v}{\partial y})-w_2 f_y\}dxdy-\oint_{\Gamma^e} w_2 t_y ds
\end{aligned}
\tag{4.8}
$$

where t_x and t_y denote the boundary forces defined in Eqs. (4.7).

Using the finite element interpolation of the form of the displacement u and v, and substituting $w_1 = \psi_i$ and into Eqs. (4.8), we obtain

$$
\begin{aligned}
[K^{11}]\{u\}+[K^{12}]\{v\} &= \{F^1\} \\
[K^{21}]\{u\}+[K^{22}]\{v\} &= \{F^2\}
\end{aligned}
\tag{4.9}
$$

where

$$
\begin{aligned}
K_{ij}^{11} &= \int_{\Omega^e}(c_{11}\frac{\partial \psi_i}{\partial x}\frac{\partial \psi_j}{\partial x}+c_{33}\frac{\partial \psi_i}{\partial y}\frac{\partial \psi_j}{\partial y})dxdy \\
K_{ij}^{12} &= K_{ji}^{21} = \int_{\Omega^e}(c_{12}\frac{\partial \psi_i}{\partial x}\frac{\partial \psi_j}{\partial y}+c_{33}\frac{\partial \psi_i}{\partial y}\frac{\partial \psi_j}{\partial x})dxdy \\
K_{ij}^{22} &= \int_{\Omega^e}(c_{33}\frac{\partial \psi_i}{\partial x}\frac{\partial \psi_j}{\partial x}+c_{22}\frac{\partial \psi_i}{\partial y}\frac{\partial \psi_j}{\partial y})dxdy \\
F_i^1 &= \int_{\Omega^e}\psi_i f_x dxdy+\oint_{\Gamma^e}\psi_i t_x ds \\
F_i^2 &= \int_{\Omega^e}\psi_i f_y dxdy+\oint_{\Gamma^e}\psi_i t_y ds
\end{aligned}
\tag{4.10}
$$

4.3.3 Stress Analysis on Frame

Comparing the thickness of the plate with other dimensions, it can be defined as a plane stress problem. In order to get an optical mesh, a UNIX based computer software -- Integrated Design Engineering Assistant System , known as I-Deas, is used to generate the mesh according to the geometry profiles of the plate. After the program generated the mesh, an output file is saved for further analysis. In this case, the plate was divided into 1,312 quadrangular elements with 1,415 nodes (Fig. 4.9). The meshes near the holes are denser than other part of the plate. Because hole usually will cause stress concentration, denser mesh can get more accurate result. The stress analysis software ANSYS is used to solve the problem. Before it starts to solve the problem, the boundary condition should be defined. The plate has 750 lb. applied load on the loading edge, and fixed at the bolt holes. There are 8 nodes along the loading edge, so each node shares 95 lb. load. The nodes along the bolt holes are fixed, that means no local movement on these nodes ($u_x = u_y = 0$). According to these boundary conditions, the program computes the stresses of each element and displacement of each node.

Fig. 4.10~Fig. 4.12 represent the plots of stresses result. In Fig. 4.10, we can see the maximum tension stresses occurred on element No.186 (9453 psi). In Fig. 4.11, the maximum y direction stresses are located on element No. 267 (5010 psi). The principal stresses σ_1, σ_2 and σ_3 are also calculated. The equivalent stresses $\sigma = \sqrt{\frac{(\sigma_1 - \sigma_2)^2 + (\sigma_2 - \sigma_3)^2 + (\sigma_3 - \sigma_1)^2}{2}}$ are shown in Fig. 4.12. The maximum equivalent stress is on element No. 267 (10,006 psi). The yield tension stress of the material are 40,000 psi. So the part is loaded far below the material limit.

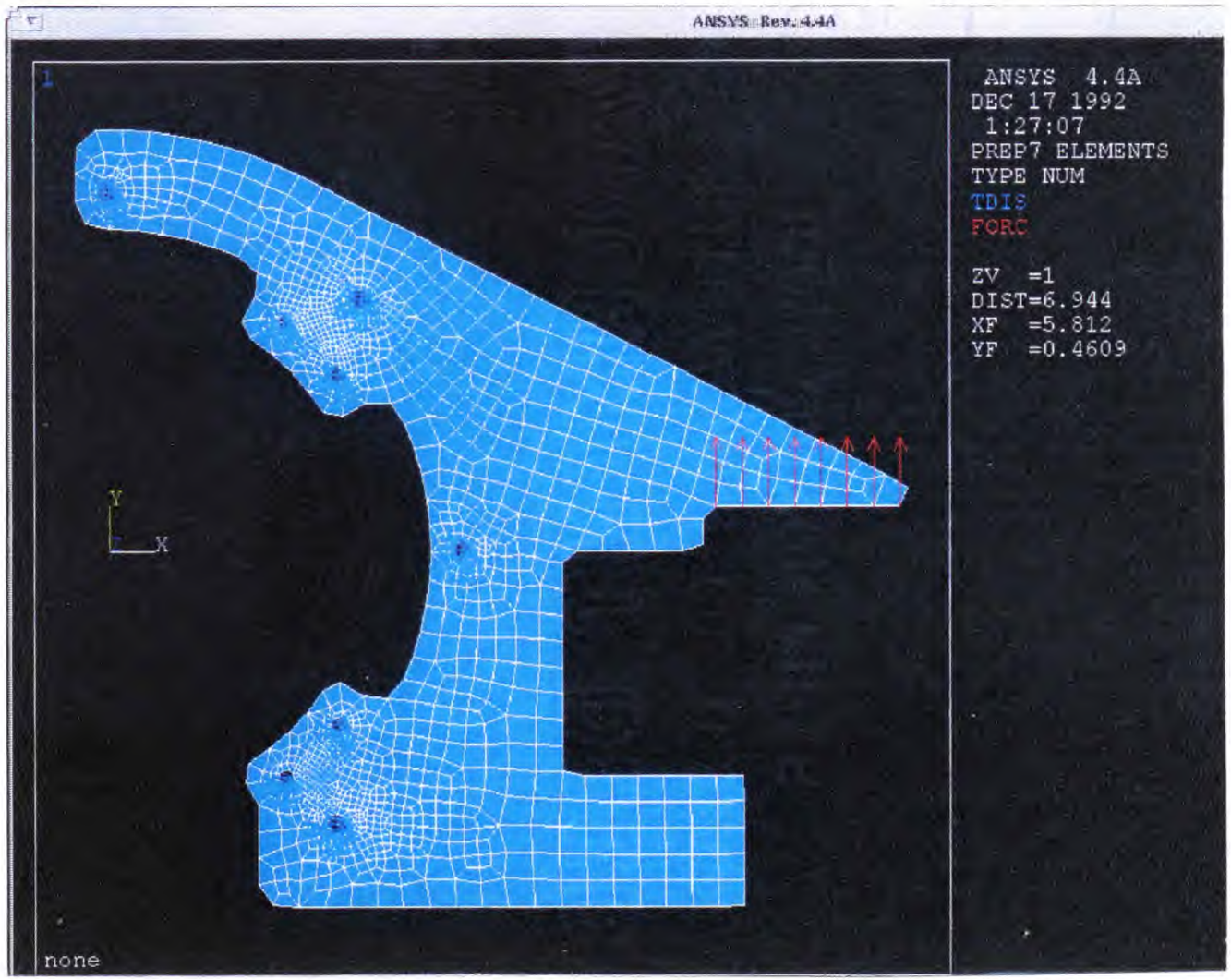

Fig. 4.9 Elements and nodes

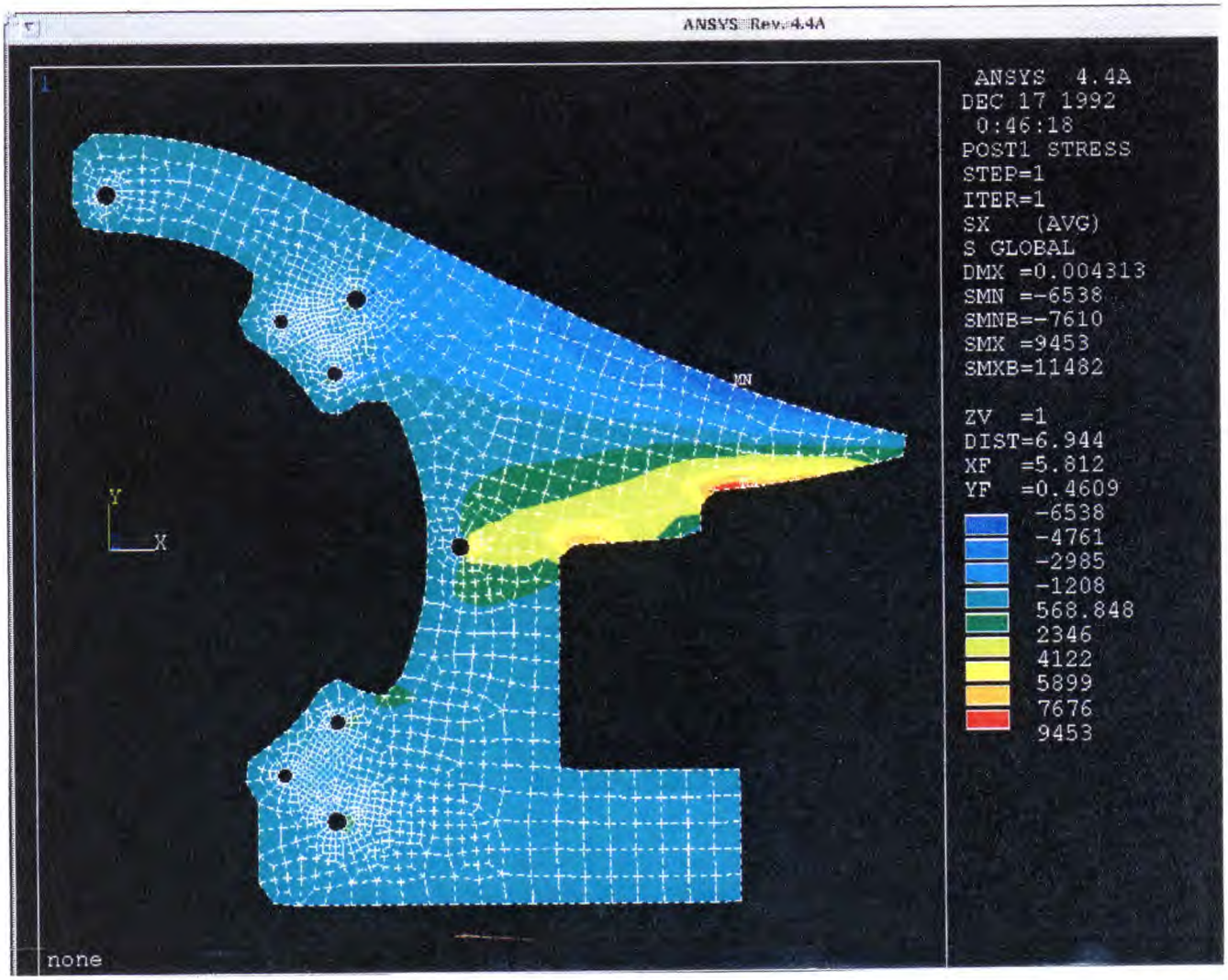

Fig. 4.10 Stresses in X-direction

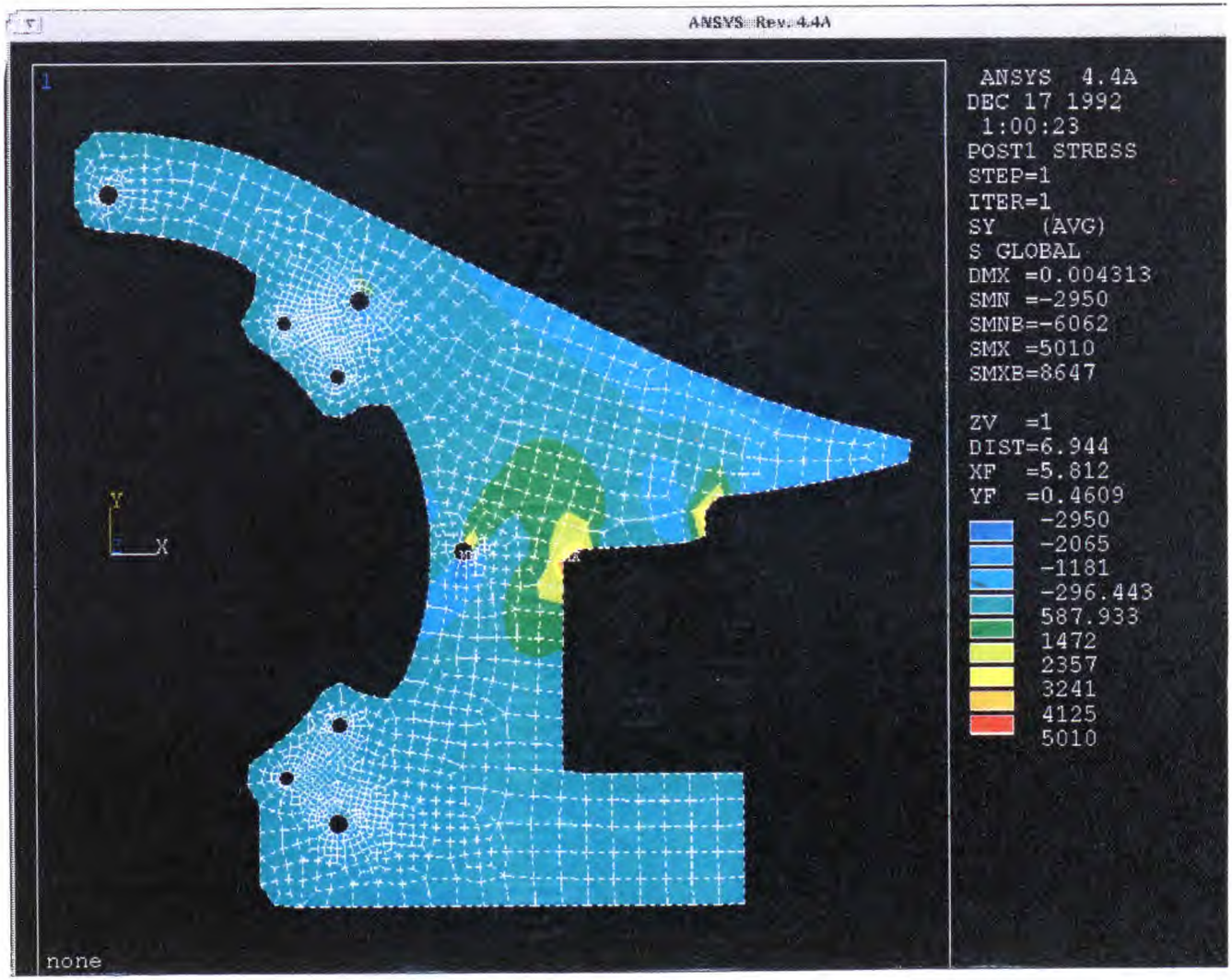

Fig. 4.11 Stresses in Y-direction

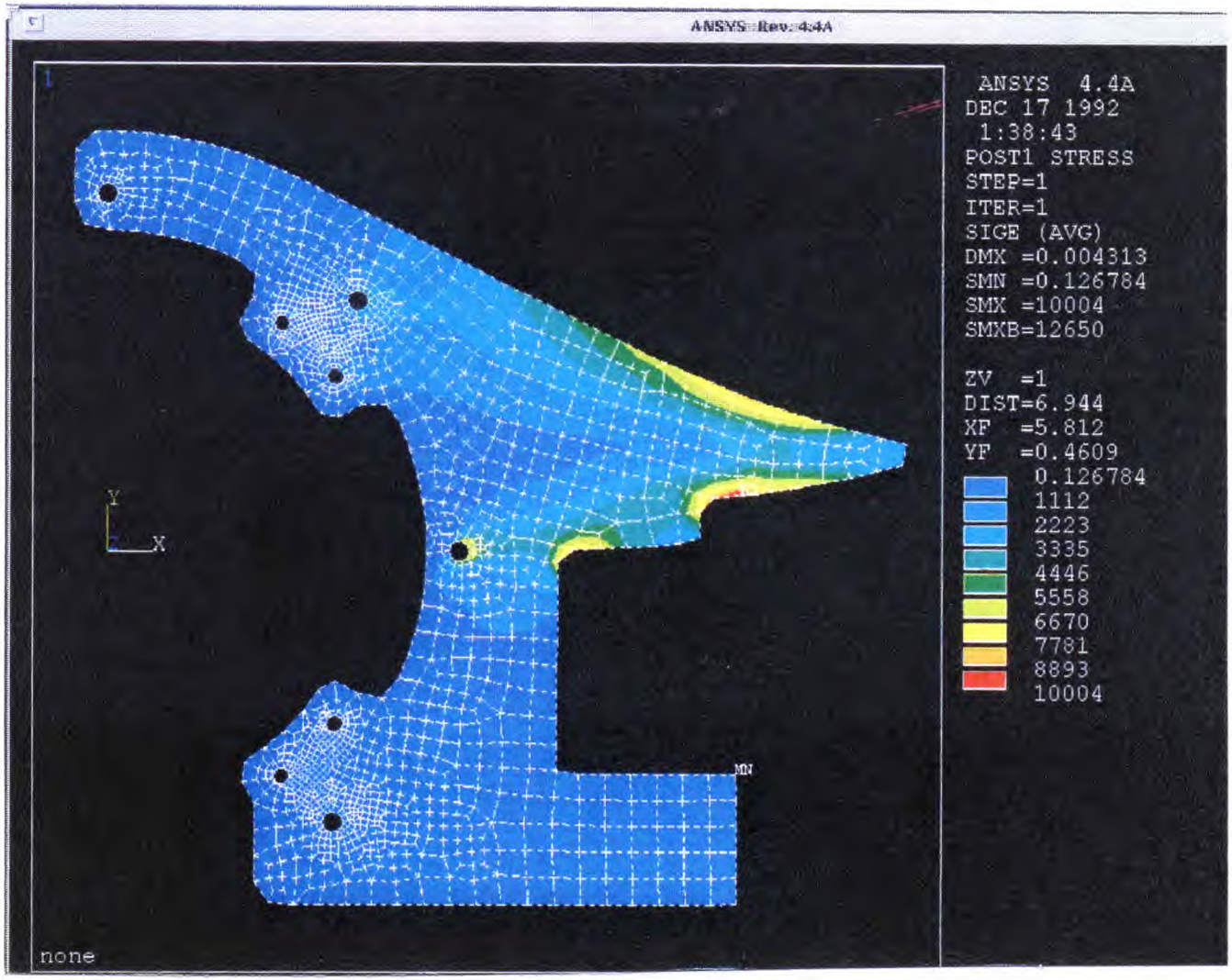

Fig. 4.12 Equivalent stresses

CHAPTER 5

EXPERIMENTAL RESULTS AND DISCUSSION

5.1 Material and Treatment of Specimens

There are two kinds of tool steel AISI H13 and D2 used in wear resistance test. Following two treatment processes are used to treat the test specimens.

5.1.1 Ion-Nitriding Coating

Ion nitriding is a combination of vacuum coating technology and heat treating. When a high voltage is established between two electrodes in a vacuum and a small amount of a gas is introduced, a plasma can be created between the electrodes. The ions are accelerated by the potential between the electrodes and strike the cathode. In ion nitriding, the work is cathode and the steel chamber of a vacuum furnace is the anode. The work is insulated from the chamber such that the only way that current can flow between the work and the chamber walls is through the ionized gas in the chamber (Fig. 5.1).

The specimens to be ion nitrided should be cleaned and placed on a work support that is insulated from all other parts of the system but is electrically connected to the power supply. Specimens are spaced so that they do not touch each other, and the charge is stacked symmetrically. The chamber is pumped down to about 3 to 5 torr. The specimen may then be cleaned by introduction of hydrogen or some other gas into the chamber. The impinging ions remove oxides and other surface contaminants from the work. The nitriding process is commenced by feeding nitrogen gas into the chamber, and a potential from 400 to 1000 volts DC is established between the chamber and the work. A plasma glow

is established around the specimens, and they will be heated up to the range of 550° to 650°C nitriding temperature. The glow is maintained during the nitriding cycle.

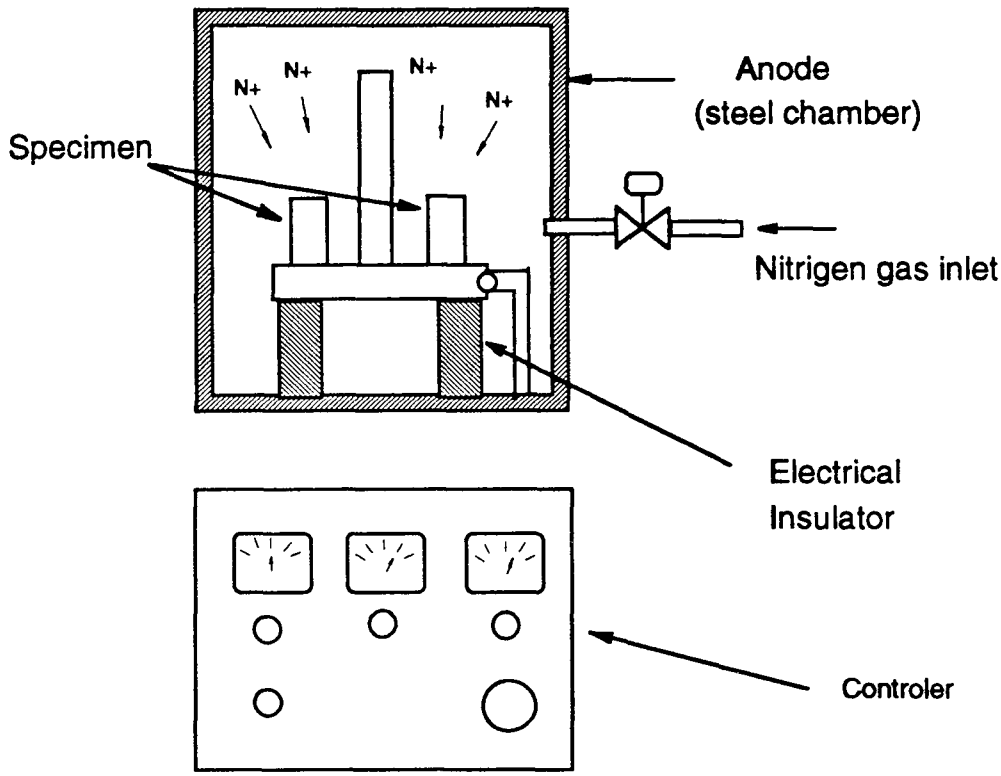

Fig. 5.1 Schematic of Plasma Ion-Nitriding.

Different temperature and pressure combinations are used for the optimization[19]. Three group of specimen has been treated under different gas composition at 650°C.

Table 5.1 Gas composition used for specimen treatment

Gas Composition	Group A	Group B	Group C
N_2	65%	25%	5%
H_2	35%	75%	95%

5.1.2 Magnetization

Selected materials are magnetized in a magnetic field[18]. In this work, the effect of magnetization on wear resistance of tool steel has be tested. The different groups of specimens have been magnetically treated before or after being plasma ion-nitrided. The specimens were put in an insulated magnetic device with the magnetic field oriented perpendicularly to the test surface. Every magnetic cycle is followed by a demagnetization cycle. 5 cycles or 30 cycles have been done on each group of specimens before or after the ion-nitriding process.

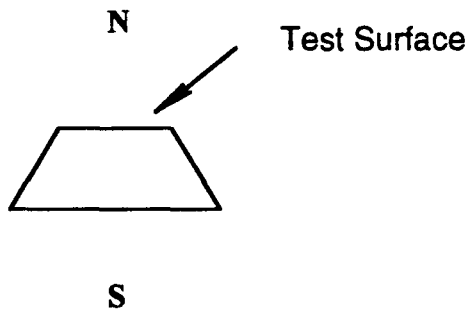

Fig. 5.2 Applied magnetic field.

5.2 Friction Coefficient

The wear occurs when two surfaces come to contact and have relative motion. There are three stages of wear: running in stage, steady stage, and catastrophic wear. In the running in stage the friction force changes from zero to a higher value than it goes down to a normal value which represents the steady stage. When the friction force suddenly increases in catastrophic stage, the surface of the specimen is destroyed producing catastrophic wear. The friction force jumps up and down becoming irregular in this stage.

The friction forces vs. sliding distances are plotted in Fig. 5.3, Fig. 5.4 and Fig. 5.5. The tested specimens are manufactured from AISI H13 tool steel and treated by ion nitriding. In Fig. 5.3 for specimen pre-magnetized by 20 cycles, the friction force turns irregular after 4,600 seconds of operation. If the specimen is pre-magnetized with 40 cycles treatment the friction force turns irregular after 9,000 seconds of operation (Fig. 5.4). The specimen pre-magnetized with 60 cycle treatment didn't show this damage even after 10,400 second of operation (Fig. 5.5).

5.3 Surface Roughness

The values of R_a, the average roughness of specimens, are calculated and plotted out for comparison. When the surface is damaged the value of R_a goes to very high numbers. Fig. 5.6 shows the surface roughness change for H13 tool steel specimen without any treatment. And it is found that the surface is totally destroyed after 15 minutes of operation. At the same time the surface of the same material after magnetic and nitriding treatment keeps in good condition after 180 minutes of operation (Fig. 5.7).

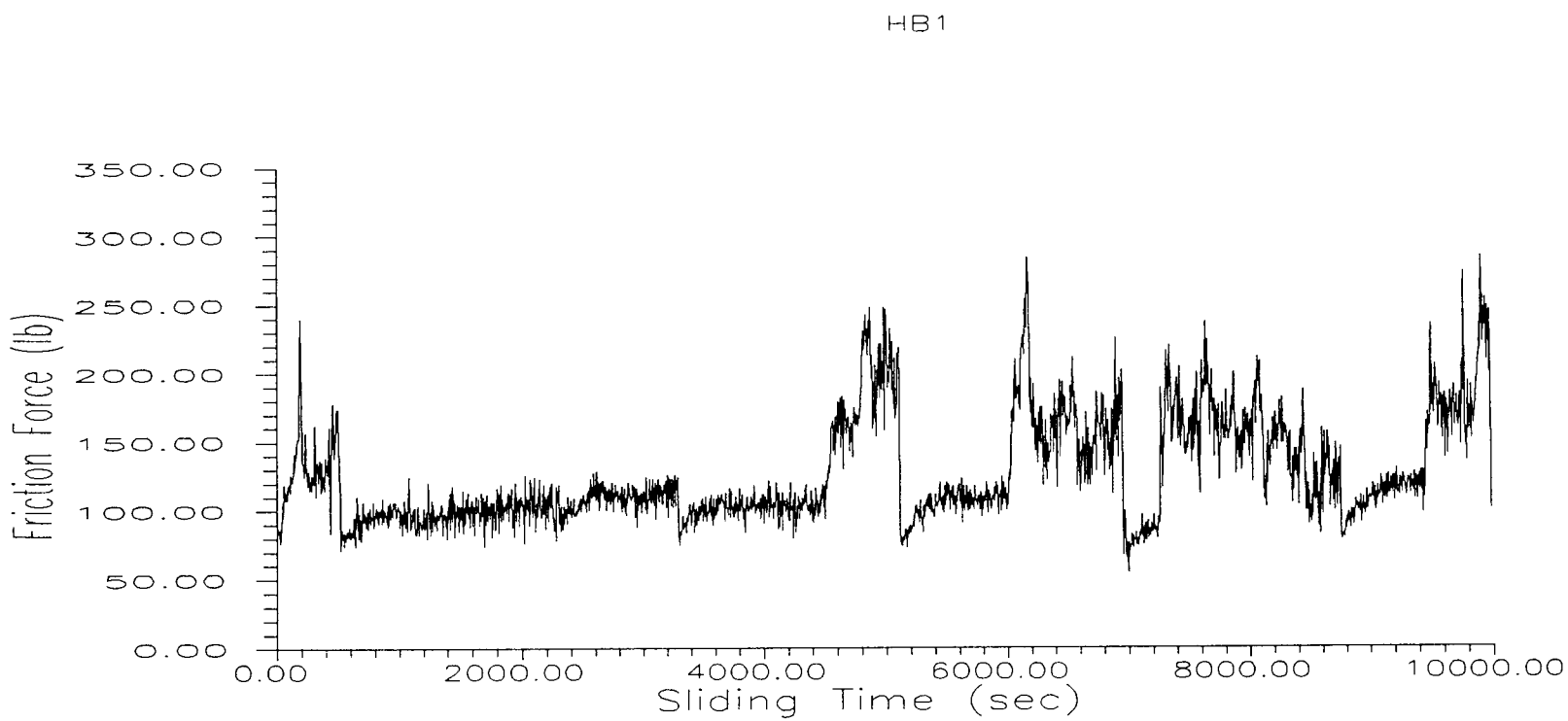

Fig. 5.3 Relationship of friction force and sliding time of H13 tool steel with 20 cycles of pre-magnetize treatment

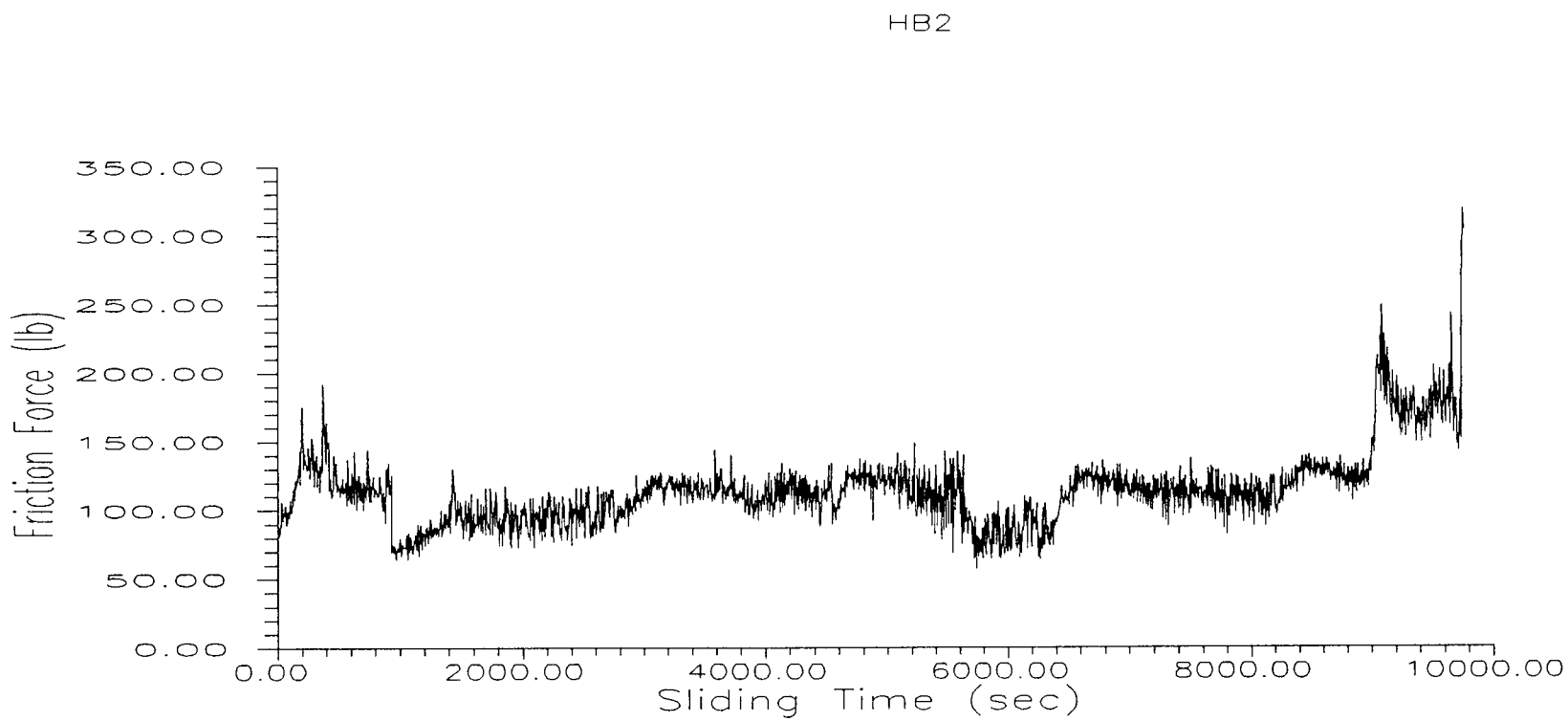

Fig. 5.4 Relationship of friction force and sliding time of H13 tool steel with 40 cycles of pre-magnetize treatment

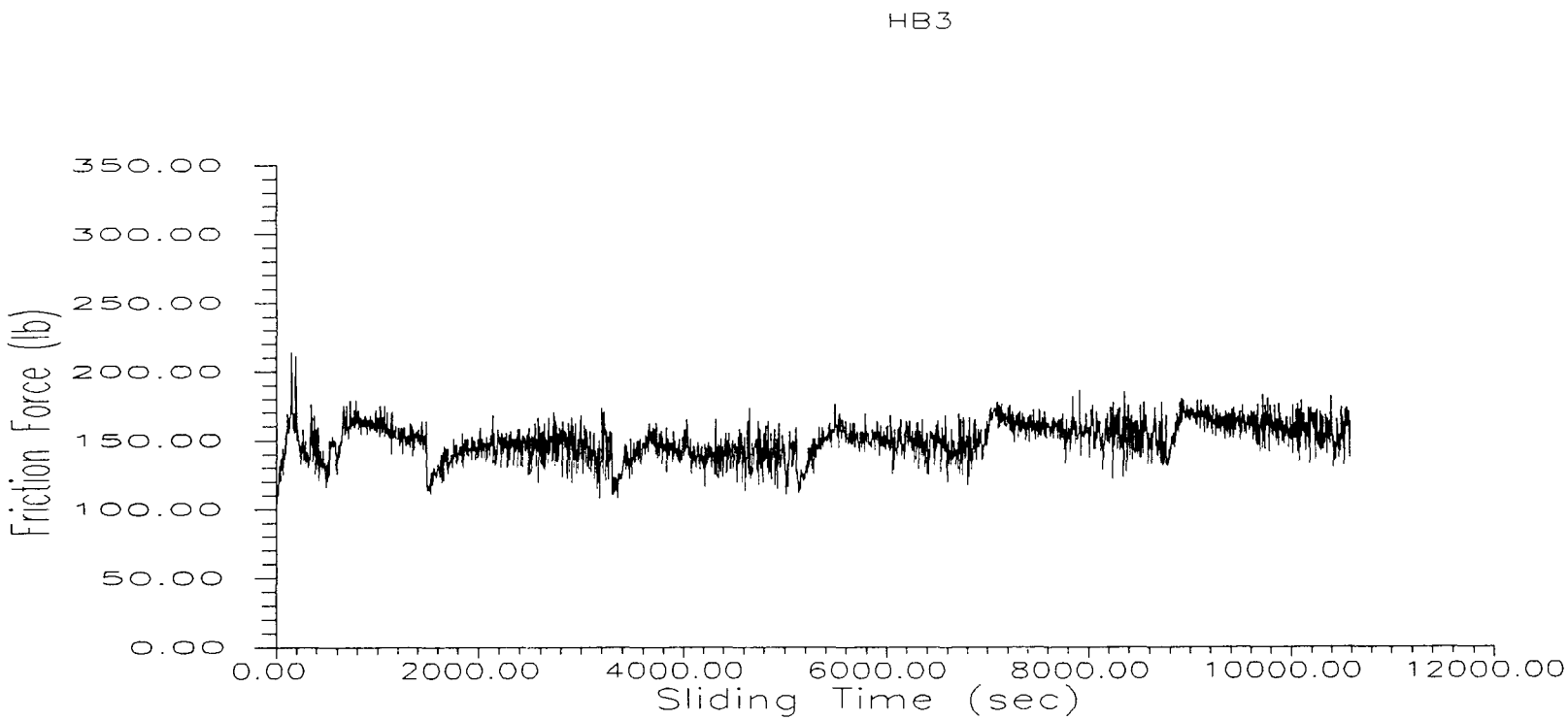

Fig. 5.5 Relationship of friction force and sliding time for H13 tool steel with 60 cycles of pre-magnetize treatment

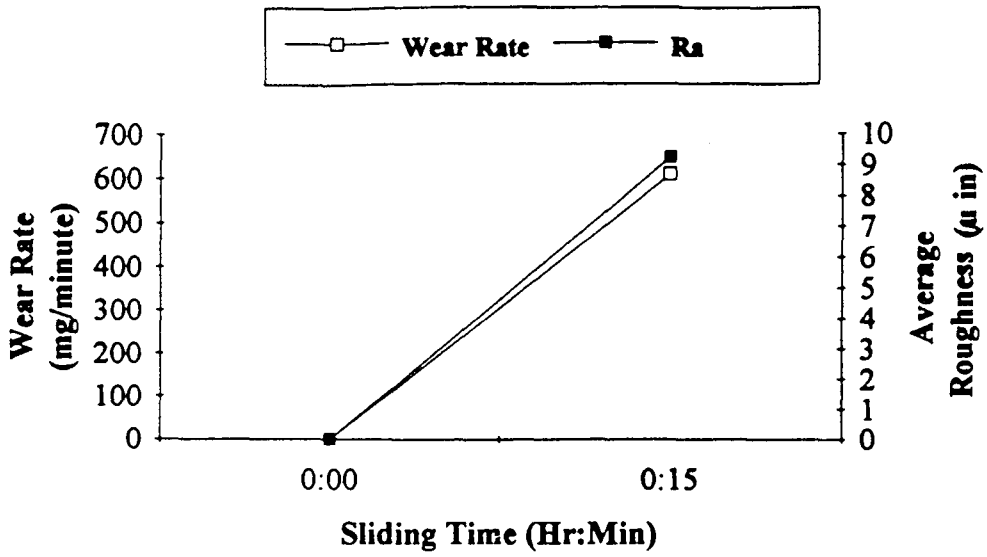

Fig. 5.6 Wear rate and average roughness of H13 tool steel without any treatment.

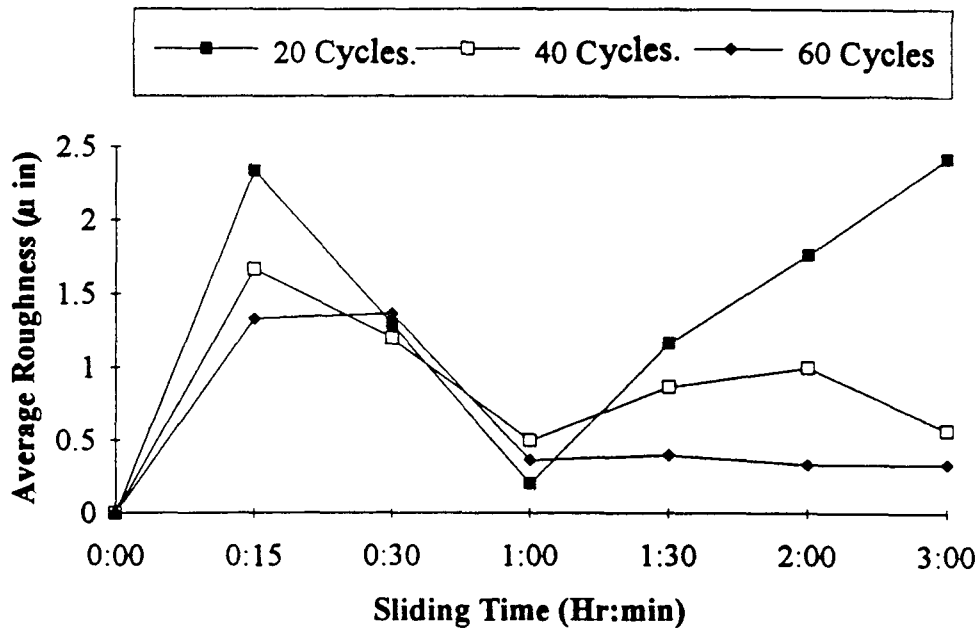

Fig. 5.7 Average surface roughness for H13 tool steel ion-nitrided and pre-magnetized with different cycles.

5.4 Wear Rate

Specimens made from AISI H13 tool steel have been employed for complete wear resistant analysis. Gas concentrations and type of treatment used in this wear test are listed in Table 5.2.

Table 5.2 Gas Composition and Type of Treatments

Gas composition	Non-Magnetized	Magnetized before Nitriding		Magnetized after Nitriding	
N_2:H_2		30 cycles	5 cycles	30 cycles	5 cycles
65:35	X	X	X	X	X
25:75	X	X	X	X	X
5:95	X	X	X	X	X

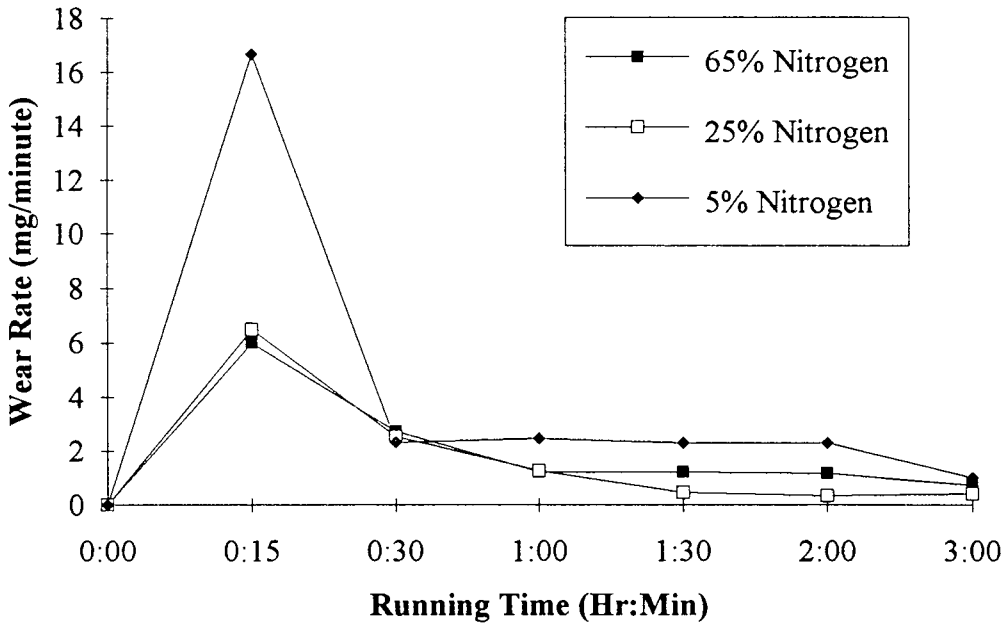

Fig. 5.8 Wear rate of AISI H13 tool steel treated in atmosphere with different nitrogen concentration.

Fig. 5.8 shows wear rate of AISI H13 tool steel nitrided without any other treatment. Treatment of specimens in atmosphere with 65% and 25% nitrogen concentration didn't make big difference on wear rate. Specimen treated in atmosphere with 5% N_2 concentration has very high wear rate. Fig. 5.9 shows H13 steel nitrided at different gas concentration with 5 cycles pre-magnetize treatment. The 5% N_2 concentration treated specimen still has the highest wear rate, but specimen treated at 25% N_2 concentration has a higher wear rate in comparing with specimen treated at 65% N_2 concentration. These two figures show the tendency that the higher nitrogen concentration provides the lower wear rate in spite of the magnetic treatment.

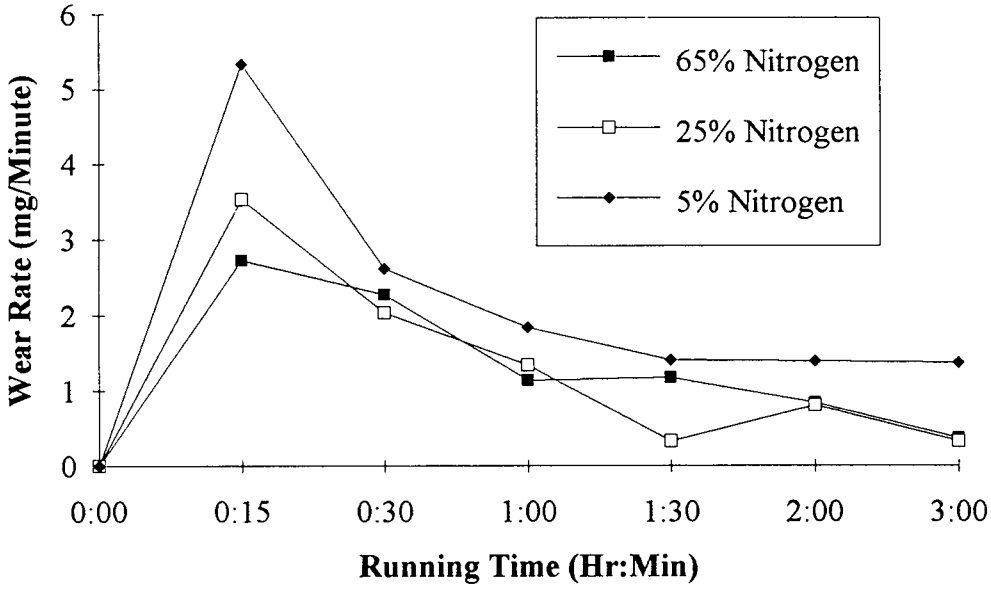

Fig. 5.9 Ware rate of AISI H13 tool steel treated at different nitrogen concentration along with pre-magnetic treatment.

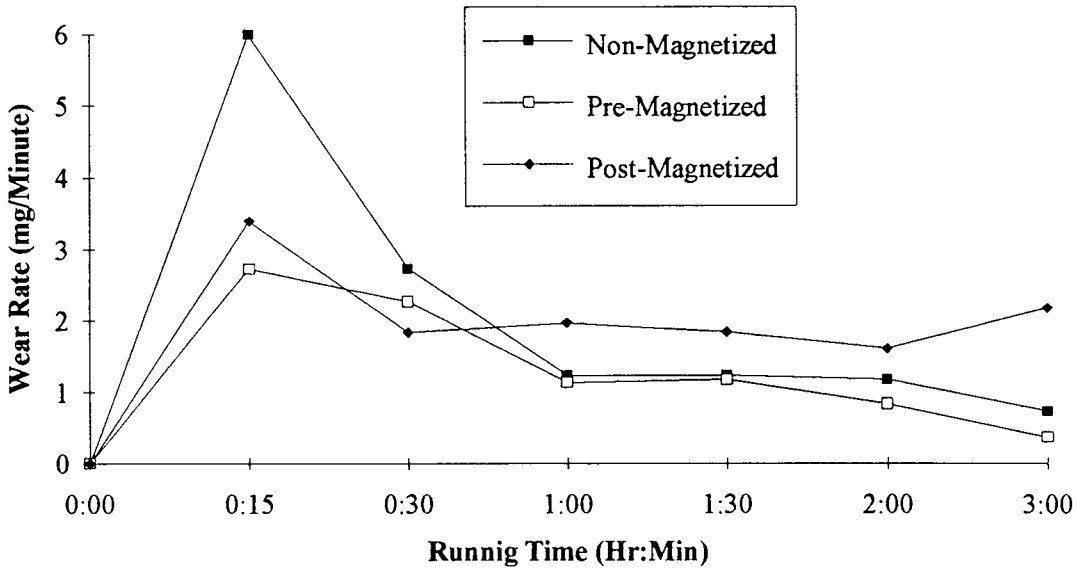

Fig. 5.10 Wear rate of AISI H13 tool steel treated in 65% nitrogen concentration atmosphere and 5 cycles of pre or post magnetize treatment.

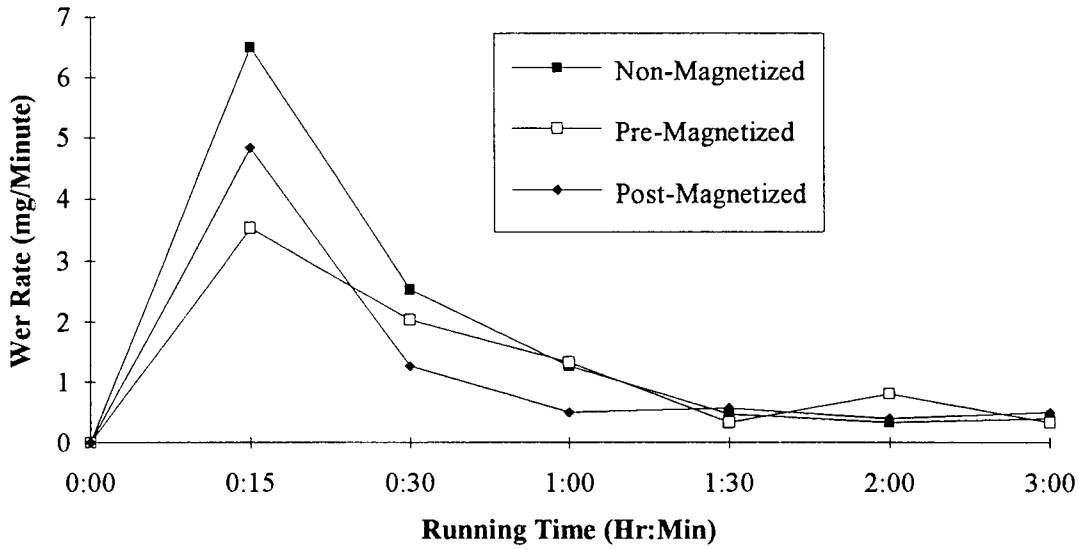

Fig. 5.11 Wear rate of AISI H13 tool steel treated in 25% nitrogen concentration and with or without 5 cycles of magnetize treatment.

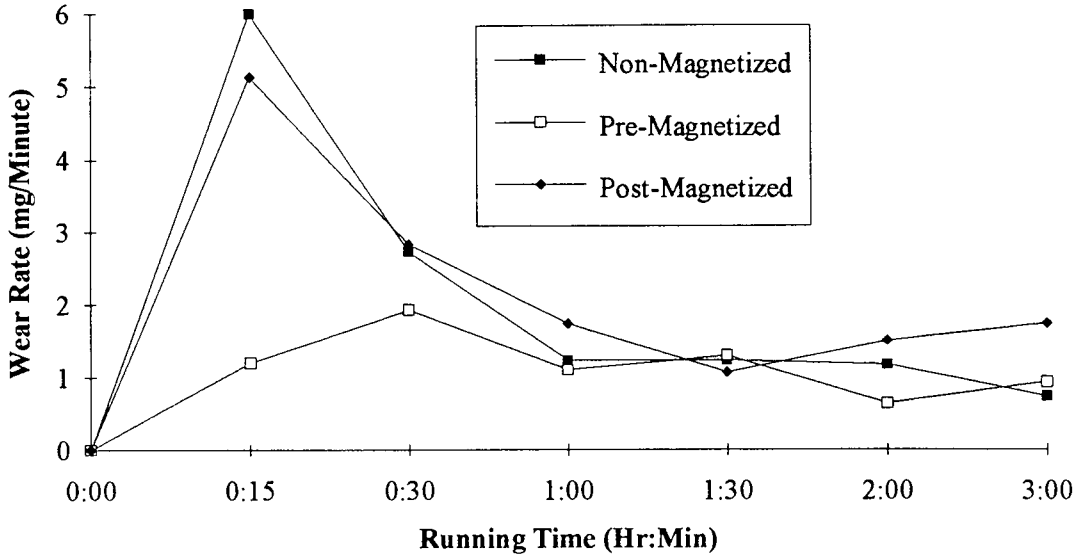

Fig. 5.12 Wear rate of AISI H13 tool steel treated in 65% nitrogen concentration and with or without 30 cycles of magnetize treatment.

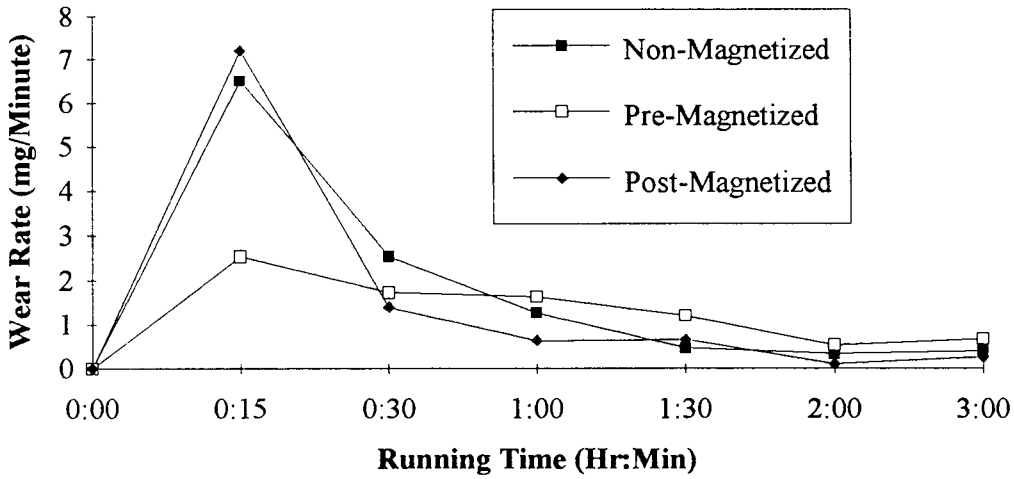

Fig. 5.13 Wear rate of AISI H13 tool steel treated in 25% nitrogen concentration and with or without 30 cycles of magnetize treatment.

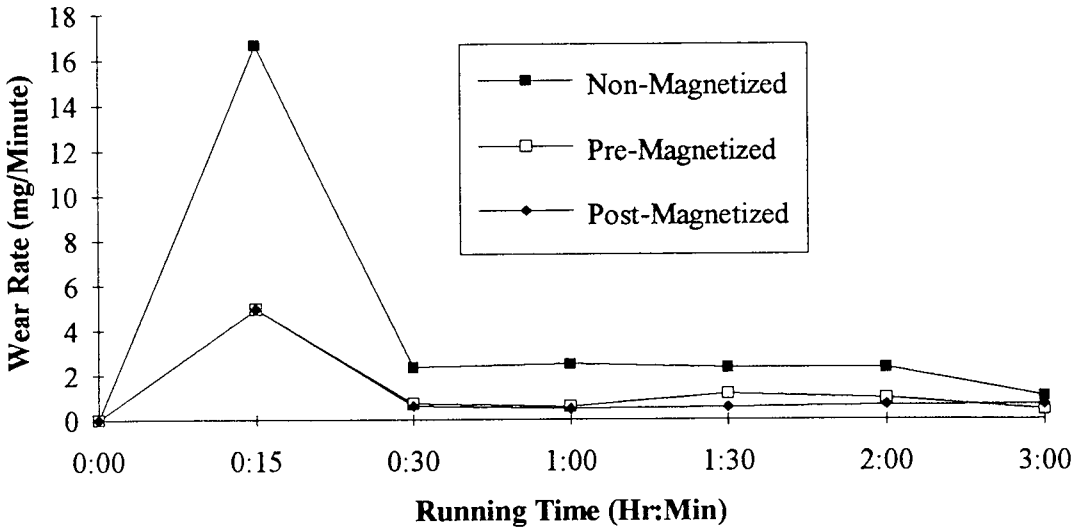

Fig. 5.14 Wear rate of AISI H13 tool steel treated in 5% nitrogen concentration and with or without 30 cycles of magnetize treatment.

In Fig. 5.10 to Fig. 5.14, the effect of magnetic treatment on wear rate is shown. As you can see, from Fig. 5.10, the non-magnetized specimen has twice the wear rate of magnetized one. Wear Rate of pre-magnetized specimen is lower than that of post-magnetized specimen. Specimen nitrided at 25% N_2 concentration with 5 pre-magnetize cycles (Fig. 5.11) shows better wear resistance than post-treated one. The non-magnetized specimen has twice higher wear rate than the pre-magnetized. When the amount of magnetize cycles is raised to 30, the specimen treated by 65% N_2 concentration shows a steady, flat low wear rate. At the same time the post-treated specimens exhibit a higher wear rate than that for the pre-magnetized but lower than that for the non-treated specimen (Fig. 5.12). The wear rates of the non-magnetized, pre-magnetized and post-magnetized samples treated by 25% N_2 (Fig. 5.13) show the same order as the wear rates of the specimens treated by 65% N_2 concentration. When the N_2 concentration drops

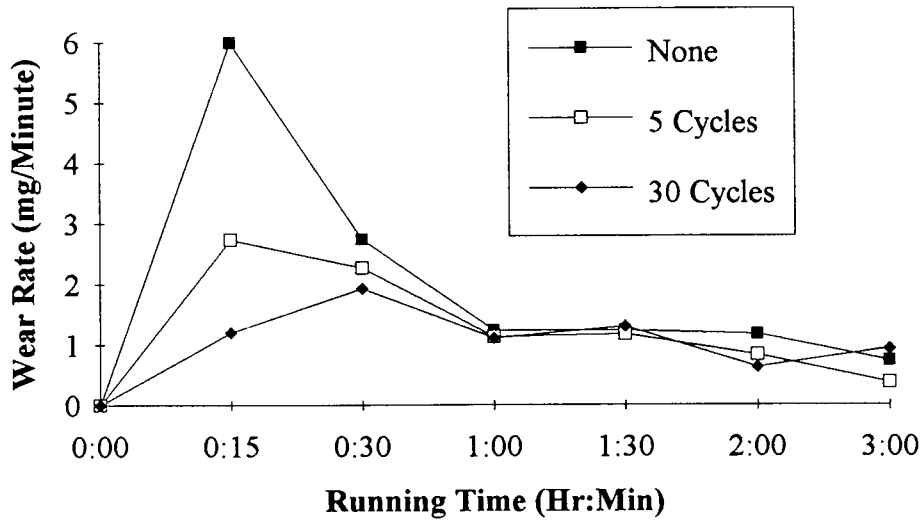

Fig. 5.15 Wear rate of AISI H13 tool steel treated at 65% nitrogen concentration with or without different pre-magnetize treatment.

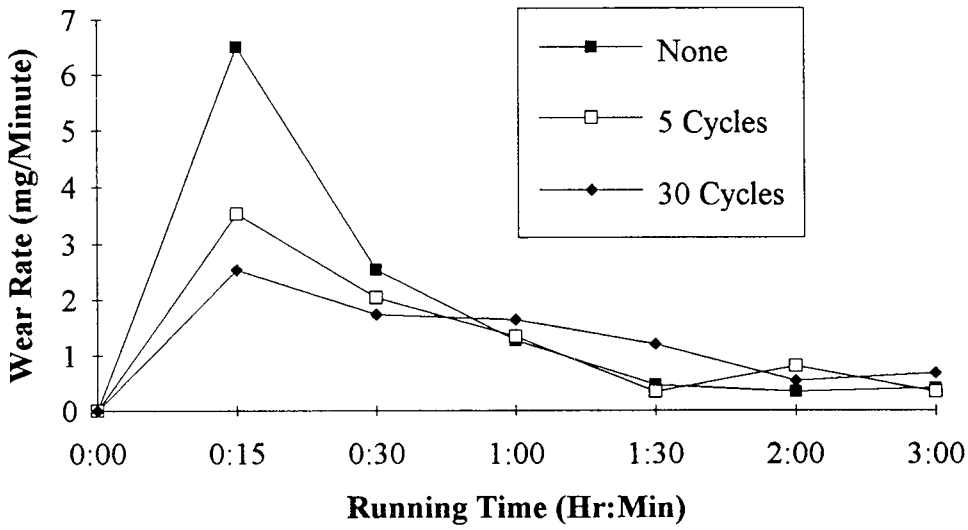

Fig. 5.16 Wear rate of AISI H13 tool steel treated at 25% nitrogen concentration with or without different pre-magnetize treatment.

to 5%, the pre-treated and post-treated specimens have very close wear rate. The wear rate of non magnetized specimen goes up high (Fig. 5.14). The tendency is that pre-magnetic treatment improves the wear resistance better than the post-magnetic treatment. As can be seen from Fig. 5.15, the specimen treated by 65% nitrogen and with 30 magnetic cycles has the lowest and steady wear rate, the non-treated specimen has the highest wear rate, and the specimen treated by 5 cycles has the wear rate in between. The wear rate decreases with the increasing of number if cycles of magnetic treatment. Specimens nitrided at 25% of nitrogen concentration and premagnetized show the same wear rate as the specimens treated at 65% nitrogen concentration (Fig. 5.16).

CHAPTER 6
CONCLUSIONS

In this work a roller-on-roller wear testing machine is modified, manufactured, and assembled. Wear testings have been done on the selected and differently treated AISI tool steel specimens by using existing computer controlled wear testing machine.

As a result of this work, loading mechanism is designed for a roller-on-roller wear testing machine. A special frame assembly has been designed, manufactured and mounted by the existing bolts on the gearbox to convert a vertical linear motion of the pushing up mechanism into a horizontal motion of the output shaft of gearbox I, in order to load the two testing rollers.

Load cell assembly is designed and is inserted into the loading mechanism between the frame assembly and pushing up mechanism, in order to pick up the load information during the test. Special plates and handles have been used to hold the load cell and easy place it in and take it out during the loading and unloading.

Special steel bearing bases are designed and manufactured to replace the original cast iron pillow block bearings to withstand a maximum applied load.

A special seamless ball top pusher is designed to replace the ball top screw providing a stable and self-alignment contact between the pushing up mechanism and load cell assembly.

Pushing up mechanism is readjusted and slider length is corrected.

The finite element stress analysis has been done on the plate of the frame assembly for reliability check. The Integrated Design Engineering Assistant System, known as I-Deas is used to generate the mesh of the part and a UNIX

based stress analysis package -- ANSYS is employed to calculate and plot the stresses distribution.

More than 30 specimens of AISI H13 and D2 tool steels nitrided under different nitrogen concentration and/or treated by different magnetic cycles are tested for wear resistance on a computer controlled wear testing machine.

Friction force has been calculated during all the periods of test by monitoring the torque. Friction force becomes irregular when surface damadged by catastrophic wear. It has been found that the plasma ion-nitrided parts can last longer than the non-nitrided parts. And the pre-magnetized and nitrided specimens can last even longer than the pure nitrided parts. The larger the number of pre-magnetic cycles is used in the magnetic treatment the higher the wear resistance is.

The wear rates of the parts are measured and analyzed at every 15 minutes in the first half hour and then every half hour. It is found that the nitrided parts have lower wear rates than the non-treated parts. The magnetized and nitrided parts have lower wear rates than the pure nitrided parts. The pre-magnetized and nitrided parts have lower wear rates than the post-magnetized and nitrided parts. Within the pre-magnetized and nitrided parts, when the number of magnetic cycles increase the wear rate decreases. Same thing happens on the parts in the post-magnetized and nitrided group.

The surface roughness of the testing specimens has been observed by using a Sufanalyzer 4000 unit and a Dell computer unit. The roughness data were taken every 15 minutes in the first half hour and later on once every 30 minutes. The test results show that the nitrided and magnetized surfaces have better surface quality than that of non-treated surfaces after same time of operation. Generally, if specimens are treated by more number of magnetic cycles the surface roughness is lower.

WORKS CITED

1. G-40, *Annual Book of ASTM Standards,* Section 02, Vol. 03 (1987).

2. Siebel, E. "Uber die praktische Bewahrung dermit verschlebicer suchen gewonnenen Ergebnisse." *J. T. Tagunsband,* VDI-Verschleibtagung, Stuttgart (1981).

3. Burwell, J.T. "Survey of Possible Wear Mechanisms." *Wear,* Vol. 1 (1957): 119-141.

4. Buhushan, B. "The real Area of Contact in Polymeric Magnetic media: II, Experimental Data and Analysis", *ASLE Trans.* Vol 28 (1985): 181-197.

5. Keller, D.V. "Adhension Between Solid Metals." *Wear,* Vol.6 (1963): 353-365.

6. Gane, N., P.F. Pfaelzer, and D. Tabor. "Adhesion between Clean Surfaces at Light Loads." *Proc. R. Soc. Lond.* Vol. A340 (1974): 495-517.

7. Eyre, T. S. "Wear Characteristics of Metals." *Tribology Int.* Vol. 9: 203-212.

8. Neale, M. J. *Tribology Handbook.* Halsted Press, New York (1973).

9. Anonymous. "Fretting and Fretting Corrosion." *Lubrication,* Vol. 141 (1955): 85-96.

10. Dubrovsky, R., Y. Kin, and I. Shih. "Development of the Computer Controlled Wear Test Methodology." *Proc. IAMSDC-1,* TN (1989): 57.1-57.4.

11. Dubrovsky, R., and I. Shih, "Development of the Computer Controlled Seizure Test Methodology." *MRS* (1988): 140.

12 Waterhouse, R.B. "Fretting Wear." *Wear* , Vol. 100 (1984): 107-118.

13. Jahanmir, S. "On the Wear Mechanisms and the Wear Equations." *Fundamentals of Tribology,* Cambridge, MA, the MIT Press, 1978.

14. Zhou, G. Y., M.C. Leu, and S.X. Dong. "Measurement and Assessment of Topography of Machined Surfaces." *Symposium on Microstructural Evolution in Metal Processing, PED.* Vol. 46, ASME Winter Annual Meeting, Dallas, TX, 1990.

15. Moore, D. F. *Principle and Application of Tribology.* Pergamon Press (1975).

16. Farooq, M. "Wear Test Methodology and Wear Test Machine Modification." *Master Thesis*, NJIT, May (1990).

17. Reddy, J. N. *An Introduction to the Finite Element Method.* McGraw-Hill, Inc. (1984).

18. Shih, I. "Study of Surface Properties Produced by Magneto-Plasma Ion Nitriding for Improving Wear Resistance." *Dissertation,* NJIT (1992).

19. Yang, Wenge. "Development of Plasma Ion Nitriding Process Parameters to Increase Durability of Machine Components." *Master Thesis,* NJIT (1991).